Critical Reviews in Environmental Science and Technology, Volume 52, Issue 9, September 2022, pp. 1561-1603
DOI: 10.1080/10643389.2020.1860406

Microbubbles and their application to ozonation in water treatment: A critical review exploring their benefit and future application

Alexander John[1], Adam Brookes[2], Irene Carra[1], Bruce Jefferson[1] and Peter Jarvis[1*]

Cranfield University, Bedfordshire, MK43 0AL

[1]Cranfield Water Science Institute, School of Water, Energy and Environment, Cranfield, MK43 0AL, UK.

[2]Anglian Water, Thorpe Wood House, Thorpe Wood, Peterborough, PE3 6SR, UK.

*Corresponding author: p.jarvis@cranfield.ac.uk

Abstract

Ozonation is a widely applied water treatment process, used for oxidation of contaminants, as well as for the disinfection of water. However, the conventional ozonation process demands a high energy requirement and deep tanks to ensure effective mass transfer and oxidation. Microbubble technologies have emerged which have the potential to improve gas-liquid contacting. Microbubbles have diameters of 1–100 µm, while conventional bubbles used in ozonation are between 2 – 6 mm. Microbubbles have many favorable characteristics that make them suitable for ozonation. In this review, the attributes of microbubbles for ozonation have been compared with those of conventional bubbles. The higher interfacial area and lower rise velocity of microbubbles compared with conventional bubbles means that ozone in the gas phase can be more efficiently transferred into the liquid phase. This is due to a higher contact time and increased contact area of the bubble with the bulk liquid. The analysis reveals that the volumetric mass transfer coefficient can be significantly enhanced through the use of microbubbles. In addition, the steady state dissolved ozone concentration was positively impacted by the use of microbubbles. Microbubbles were shown to be able to oxidize a broader range of organic compounds more quickly than for conventional bubbles. However, the review highlighted that comparison of microbubbles with conventional bubbles is not always carried

Published by Taylor & Francis. This is the Author Accepted Manuscript issued with: Creative Commons Attribution Non-Commercial License (CC:BY:NC 4.0).
The final published version (version of record) is available online at DOI:10.1080/10643389.2020.1860406. Please refer to any applicable publisher terms of use

out in a fair and consistent way with respect to reactor configuration. Requirements for future research, more consistent experimental comparisons and the steps needed to enable implementation of microbubbles have been discussed.

KEYWORDS: Microbubbles, Ozonation, Mass transfer, Water Treatment

HIGHLIGHTS:

- Extensive comparison of microbubbles with conventional bubbles for ozonation.
- Ozone mass transfer enhanced through the use of microbubbles.
- Improved micropollutant removal when using microbubble ozonation.
- Opportunities for more efficient ozone reactor design using microbubbles.

1. Introduction

Ozonation is one of the most widely used gas-liquid contacting processes in water treatment for oxidation and disinfection applications (Lim *et al.*, 2019; Merle *et al.*, 2017; Tekle-Röttering *et al.*, 2019; Wolf *et al.*, 2019). Molecular ozone is an unstable and strong oxidant that has a standard oxidation potential of 2.07 V (Muruganandham *et al.*, 2014). When

dissolved into the liquid phase, ozone rapidly undergoes self-decomposition. The self-decomposition of ozone results in the formation of a number of products and intermediates including short lived radicals such as $HO^{\bullet}$, $O_3^{\bullet-}$, $O_2^{\bullet-}$, $HO_3^{\bullet-}$ and $HO_2^{\bullet}$ (Gardoni *et al.*, 2012). One of the most desirable decomposition products is the hydroxyl radical, $HO^{\bullet}$ which is a non-selective, powerful oxidant with a standard oxidation potential of 2.8 V (Wang *et al.*, 2018). Due to the strong oxidizing ability of molecular ozone and the hydroxyl radical, ozonation is particularly effective in the removal of aromatic organic compounds (Chedeville *et al.*, 2009; Wu *et al.*, 2019), pharmaceuticals (Azuma *et al.*, 2019; Paucar *et al.*, 2018), micropollutants (Wang *et al.*, 2019), algal by-products (Wu *et al.*, 2012) and contaminants that cause water coloration (Khuntia *et al.*, 2016). In a water treatment works (WTWs), a typical ozone contactor consists of a baffled reactor split into 1 – 2 dosing chambers and > 2 reaction zones (von Gunten *et al.*, 1999). Ozone gas is supplied through diffuser plates at the base of the dosing chamber(s), producing bubbles with a size between 2 – 6 mm (Baqero-Rodriguez *et al.*, 2018; Behnisch *et al.*, 2018; Garrido-Baserba *et al.*, 2018; Terashima *et al.*, 2016) (Figure 1). Ozone contactors typically have a large footprint and deep tank depth, and therefore require significant resources, which varies depending upon the treatment objectives and water quality (Rakness *et al.*, 2018). While reactor volume changes depending on flow treated, all ozonation contactors have deep tanks, typically around 7m (Tang *et al.*, 2005; Zhang *et al.*, 2014). This depth is required in order to ensure effective mass transfer of ozone from bubbles formed using conventional diffusers.

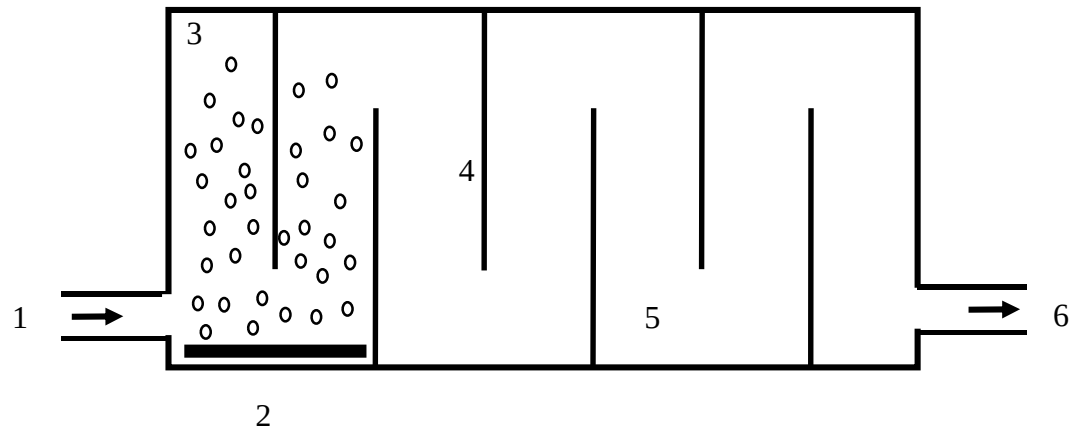

Figure 1. A typical baffled ozone contactor where (1) liquid inlet (2) diffuser plates (3) dosing chambers (4) baffles (5) reaction chambers (6) liquid outlet.

In addition to capital investment, ozonation has significant operating costs as ozone gas must be generated in-situ and cannot be stored on site due to its instability. The generation of ozone is an energy and opex intensive process with an energy demand of ~ 3.3 - 16 kWh / kg O_3 (Jodzis and Zięba, 2018; Magara *et al*., 1995). The cost of the power required to generate ozone is between 50 – 75% of the ozonation process cost (Evans *et al*., 2003) and around 15% of the total non-pumping energy requirement for a WTWs using ozone (Santana *et al*., 2014). Whilst ozone is usually delivered in the form of conventional millimeter sized bubbles, recent developments have allowed for the use of smaller bubbles known as microbubbles and nanobubbles. There has been some debate in the literature with respect to the size boundaries used to describe these small bubbles, with a range of definitions having been used (see Supplementary Information (SI) Table 1). However, since 2017 there has been a standardized definition of microbubbles and nanobubbles from the International Organization for Standardization (ISO), as being bubbles with a diameter of 1 – 100 μm and 1 – 1000 nm respectively (ISO 20480-1:2017).

Over the past few decades, interest in the application of microbubbles to water treatment has increased greatly due to their high surface area to volume ratio (Temesgen *et al*., 2017), low rising velocity (Terasaka *et al*., 2011), increased gas utilization efficiency (Zhang *et al*., 2018), increased rate of mass transfer (Wu *et al*., 2019) and increased rate of contaminant removal (Azuma *et al*., 2019). Microbubbles have the potential to decrease operational cost from a reduction in the required ozone input dose and a decreased requirement for off-gas destruction (Chu *et al*., 2008). In addition, increased treatment rates may afford opportunities for reductions in contact tank dimensions and plant footprint.

Microbubble generation has historically been considered an energy intensive process in which the cost was deemed too high to be economically viable. This was due to the high power required to produce microbubbles, using generation methods involving compression or ultrasonic cavitation (Zimmerman *et al*., 2008). Recently, however, lower powered microbubble generators have been developed. Modern developments include microbubble generators such as those produced by spherical bodies (Sadatomi *et al*., 2005), orifice plates (Sadatomi *et al*., 2012), venturis (Deendarlianto *et al*., 2017), membranes (Kukuzaki *et al*., 2010; Liu *et al*., 2012; Liu *et al*., 2013) and fluidic oscillators (Al-Mashhadani *et al*., 2015; Hanotu *et al*., 2016; Hanotu *et al*., 2017; Kamaroddin *et al*., 2016; Kamaroddin *et al*., 2020; Zimmerman *et al*., 2011a). These types of microbubble generator utilize a restriction in the fluid flow to cause a pressure drop and an automatic suction of gas (Parmar and Majumder, 2013). Many of these developments have occurred without a specific application in mind, however they now offer a more realistic opportunity for application of microbubbles in water treatment. To date, there has not been a comprehensive review of microbubbles for ozonation, despite a significant expansion of research into this application.

Accordingly, this review aims to critically review the literature to establish the current state of evidence on the potential benefits of microbubbles systems with regards to the use of ozone.

The review will explore both the mass transfer and treatment aspects of bubble size on ozone applications. The review will then consider whether full scale microbubble ozonation is a feasible option and then discuss the challenges and future perspectives associated with the use of microbubbles.

2. Mass Transfer

The transfer of gas into liquid is dependent upon the mixing conditions, the size and number of bubbles and, in the case of reactive gases such as ozone, the kinetics of decomposition (Fuchun and Cunli, 1990; Shin *et al*., 1999). The rate at which ozone gas is transferred into liquid is described through the liquid phase mass transfer coefficient and can be defined for a bubble that follows Stokes' law (Clift *et al*., 1978):

$$k_L = \frac{D_L}{d}\left[1 + \left(1 + \frac{dU}{D}\right)^{\frac{1}{3}}\right] \quad (1)$$

Where k_L is the liquid side mass transfer coefficient (m s^{-1}), D_L is the diffusivity of gas in liquid (m^2 s^{-1}), d is the bubble diameter (m) and U is the bubble rising velocity (m s^{-1}). The Stokes' equation (Talaia, 2007) is valid for particles/bubbles at low Reynolds numbers (< ~ 1) (Park *et al*., 2017):

$$U_{\infty(S)} = \frac{g d^2(\rho_l - \rho_g)}{18\mu_l} \quad (2)$$

Where $U_{\infty(S)}$ is the Stokes' terminal rising velocity (m s^{-1}), g is gravitational acceleration (m s^{-2}), d is bubble diameter (m), ρ_l is liquid density (kg m^{-3}), ρ_g is gas density (kg m^{-3}) and μ_l is dynamic viscosity of the liquid (Pa s).

When the bubble size is ≲ 100 µm the internal pressure within the bubble increases its surface rigidity leading to a reduction in frictional resistance such that the terminal rise velocity

deviates from that described by Stokes' law and is better described by the Hadamard-Rybczynski equation (Parkinson *et al.*, 2008):

$$U_{\infty(H-R)} = \frac{3}{2} U_{\infty(S)} = \frac{\rho g d^2}{12 \mu_l} \quad (3)$$

Where $U_{\infty(H-R)}$ is the Hadamard-Rybczynski terminal rising velocity (m s^{-1}).

In addition, decreases in bubble size reduces the associated buoyant force leading to a low rise velocity and hence a longer contact time such that a higher proportion of gas is retained in the bulk liquid and is not lost as off-gas (Shangguan *et al.*, 2018). It is therefore expected that this will increase the rate of mass transfer and gas utilization efficiency (Suwartha *et al.*, 2020). The larger bubble sizes associated with conventional ozonation means that the bubbles will rise quickly through the liquid and burst at the surface (Figure 2). In addition, a number of other factors impact the overall rate of mass transfer including the rate of ozone self-decomposition (Wu *et al.*, 2019), the concentration gradient between the gas phase and the steady state liquid concentration, the gas flow rate (in terms of its impact on bubble size and number density) and accumulation and surface coating of material at the bubble-liquid interface. The following considers how these factors influence the mass transfer of ozone.

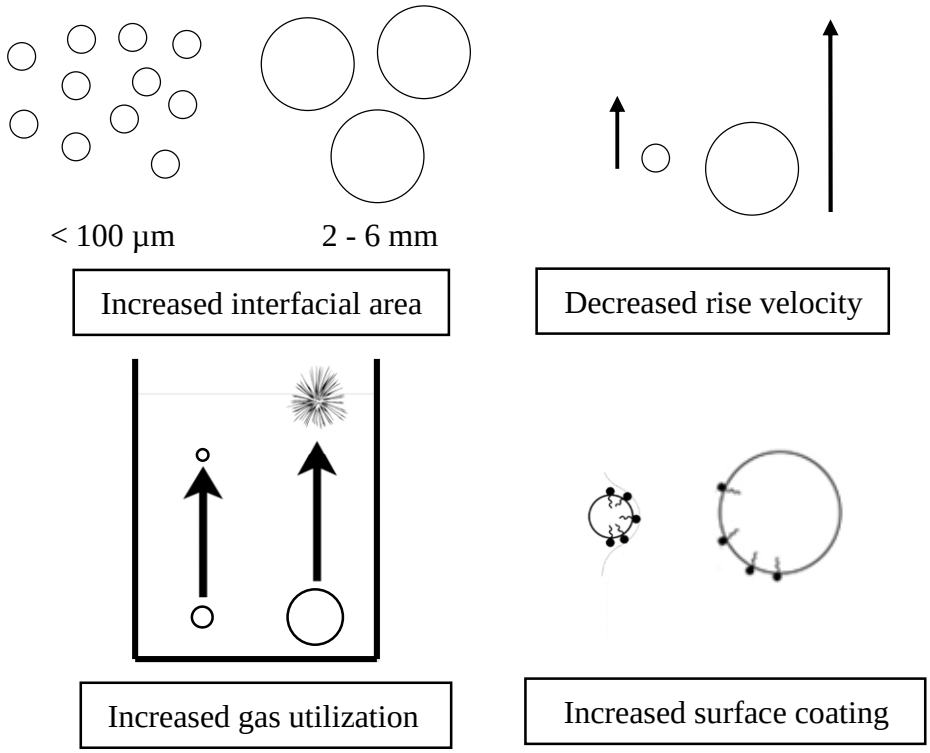

Figure 2. Notable properties of microbubbles in comparison to conventional bubbles.

2.1. *Volumetric Mass Transfer Coefficient, k_La*

The liquid side mass transfer, k_L, cannot be easily determined experimentally as in most cases the interfacial area is either unknown or cannot be reliably measured (Khuntia *et al*., 2012). However, the volumetric mass transfer coefficient, k_La, which is defined as a function of k_L and the interfacial area, a (m^{-1}), can be more easily obtained. Thus, the rate of mass transfer is often expressed in terms of k_La. The measured volumetric mass transfer coefficient is also dependent upon the rate of self-decomposition and the steady-state concentration (Wu *et al*., 2019):

$$\frac{dC}{dt} = (k_La - k_D)(C_s - C) \quad (4)$$

$$k_La^M = k_La - k_D \quad (5)$$

Where $k_L a^M$ is the measured volumetric mass transfer coefficient (min^{-1}), $k_L a$ is the actual volumetric mass transfer coefficient (min^{-1}), C_s is the steady-state dissolved ozone concentration (mg L^{-1}), C is the concentration of dissolved ozone (mg L^{-1}), and k_D is the rate of ozone self-decomposition (min^{-1}). The reporting of $k_L a$ in the literature is somewhat inconsistent with some studies reporting a measured $k_L a$ without the inclusion of k_D and other studies reporting an actual $k_L a$ including k_D in the calculation. For this reason, all of the data has been recalculated to include k_D. The actual $k_L a$ has been used if reported, and if an apparent $k_L a$ was reported, then an average k_D was applied in ensure a consistent comparison has been made (Section 2.6).

The determination of the volumetric mass transfer coefficient for ozone can be problematic due to its relative insolubility and instability in water (Huang *et al*., 1998), low rate of mass transfer and losses in the off-gas (Mitani *et al*., 2005). It is also influenced by direct and indirect reactions with pollutants (Chiu *et al*., 2003). For example, it has been established that the consumption of ozone through the reaction with contaminants can be faster than the rate of mass transfer into the water (Levanov *et al*., 2017). As such, mass transfer experiments are usually performed in deionized water at a controlled temperature where consumption by contaminants is negligible and self-decomposition is the only reaction route (Wu *et al*., 2019).

There have been several studies that have directly compared the ozone $k_L a$ for microbubbles and conventional bubbles (Gao *et al*., 2019; Nam *et al*., 2019; Shin *et al*., 1999; Wu *et al*., 2019; Xu *et al*., 2012; Zhang *et al*., 2018; Zheng *et al*., 2015). The range of $k_L a$ values reported for microbubbles at pH 7 ranged between 0.09 – 1.5 min^{-1} and between 0.1 – 1.4 min^{-1} for conventional bubbles (Figure 3). The maximum observed enhancement was 5.2 (Zhang *et al*., 2018). There were two instances where no improvement was observed. In both of these cases, the apparent $k_L a$ was extremely small and the applied k_D represented a large proportion of the total value. When the above data was aggregated and considered as a whole, the average

enhancement in k_La when comparing microbubble to conventional bubble trials was 2.5 ± 1.3 times.

From this analysis it was evident that while there was a large variation in the enhancement factors reported across different studies, microbubbles outperformed conventional systems. The microbubble enhancement factor is commonly attributed to an increase in surface area. The small size of microbubbles promotes a larger interfacial area to maximize contact between the gas and liquid (Akimov *et al.*, 2011). As an example, the interfacial area of a 25 µm bubble compared to a 2 mm bubble is 80 times higher for a given volume of gas. However, it should be noted that in most cases, the measurement and reporting of bubble diameters (especially for conventional bubbles), is not routinely carried out. In almost all cases, conventional bubble size is approximated, or not stated, so a determination of the relationship between k_La and bubble diameter is not possible.

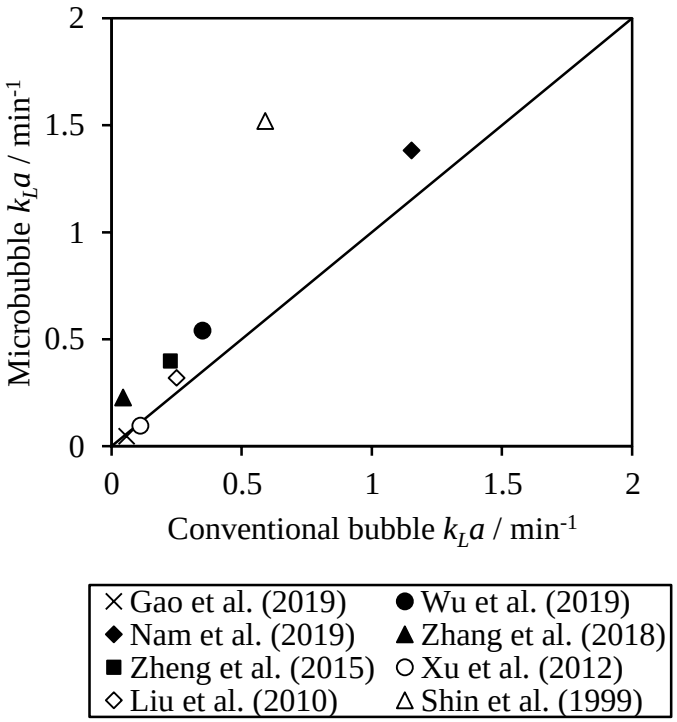

Figure 3. Volumetric mass transfer coefficient for microbubbles and conventional bubbles in direct-comparison experiments at pH 7.

Further to this, there is considerable variation in the reported k_La values between authors. This reflects variations in the systems used, both in terms of the bubbles generated with respect to their size, distribution and the experimental apparatus used to conduct the measurements. This includes differences in: the method of generating bubbles, bubble diameters and concentration, reactor geometries and liquid depths, and gas flow rates (see SI Table 2). Some of the important bubble parameters such as size and concentration are often either not reported or do not consider variable bubble size distributions. For example, we could only find one example where bubble concentration was reported in the paper (micro/nanobubble concentration between 4.35-4.63 x10^7 bubbles per mL (Hu and Xia, 2018)). It is therefore particularly difficult to compare the effects of different parameters on ozone transfer across multiple

studies. Accordingly, when comparing data across multiple studies, the underlying trends have been considered more important than consideration of absolute data values. Direct comparison between microbubble and conventional bubble systems from the same study are usually more reasonable as they are typically performed under similar experimental conditions. The following section considers how different variables influence mass transfer for both conventional and microbubble ozonation.

2.2. *Effect of pH on k_La*

In ozonation, the pH of the water is an important parameter because it influences the self-decomposition of ozone. At higher pH, ozone decomposes more quickly due to the increased amount of hydroxide ions present in the bulk solution which initiate and accelerate the self-decomposition reaction chain. The effect of changing pH is observed through the associated changes in the water chemistry with the impact seen in relation to the rate of self-decomposition (Section 2.6) and steady-state concentration (Section 2.7). Direct comparison of microbubbles and conventional bubbles at pH's other than 7 is rarely investigated (Figure 4). One example comes from Wu *et al*. (2019) who observed that the k_La increased with increasing pH from 0.34 min^{-1} at pH 3 up to 0.58 min^{-1} at pH 9 for microbubble ozonation. Lower values were seen for conventional bubble ozonation, increasing from 0.27 min^{-1} at pH 3 up to 0.37 min^{-1} at pH 9. Comparison under acidic conditions have reported enhancement factors of 1.8 at pH 2 (Chu *et al*., 2007) and 2.1 at pH 3 (Sun *et al*., 2020) when comparing microbubbles with conventional bubbles.

There have also been microbubble studies which have looked at the effect of changing pH without comparison with conventional bubble systems that indicate an enhancement in transfer coefficients under more alkaline conditions (Figure 5). The observed increase in k_La with

increasing pH has been described as a function of k_D (Khuntia *et al.*, 2013). As k_D increases with pH, the steady state dissolved ozone concentration decreases. Therefore, at high pH a steady state ozone concentration is reached faster than for a comparable low pH system. To illustrate, in a tap water study using microbubbles of < 30 µm diameter, the k_La increased from 0.30 min^{-1} to 0.41 min^{-1} as the pH increased from 6 to 9 (Jabesa and Ghosh, 2016a). This has also been observed with different ozone input concentrations where the k_La ranged from 0.10 – 0.14 min^{-1} at pH 6 to 0.16 – 0.24 min^{-1} at pH 9 for input concentrations of 329 – 1000 mg L^{-1} with a microbubble diameter of 25 µm. Increasing k_La as pH goes up is in line with expectations since k_La is directly linked to both k_D and the steady-state concentration.

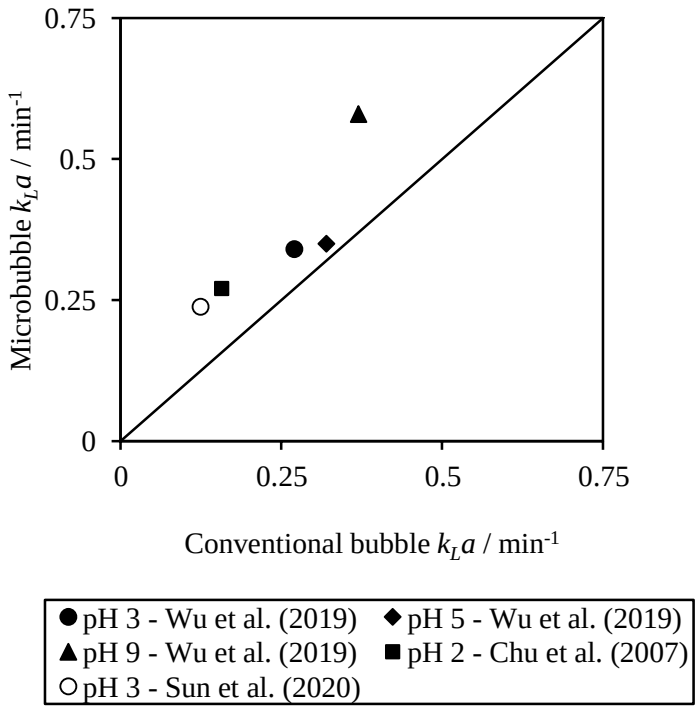

Figure 4. Volumetric mass transfer coefficient for microbubbles and conventional bubbles at varying pH's in direct-comparison experiments.

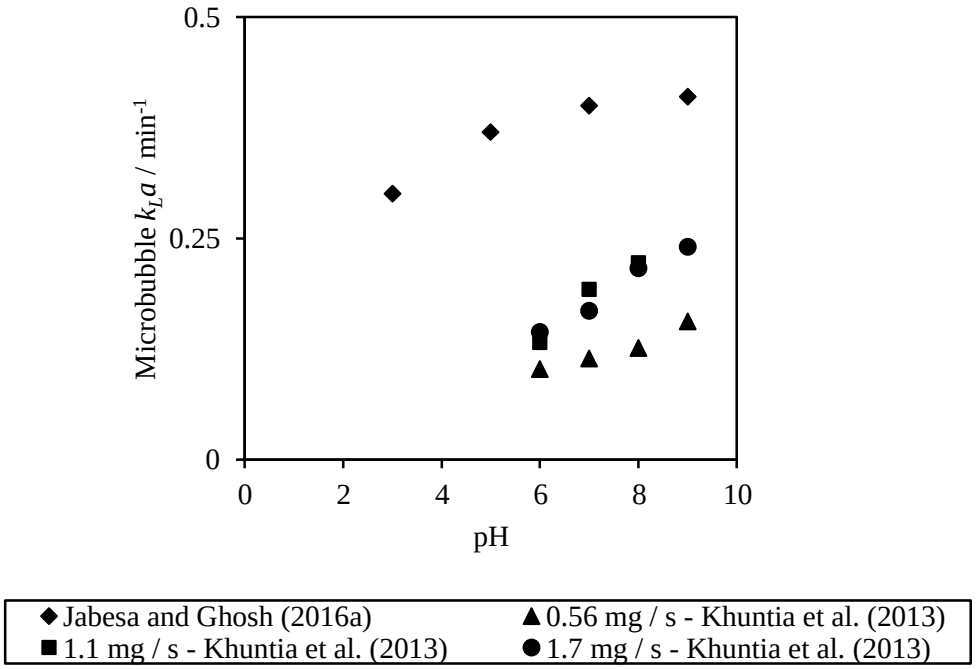

Figure 5. The change in ozone k_La for microbubbles with increasing pH.

2.3. *Effect of Ozone Input Concentration on k_La*

Increasing the concentration of ozone in the input gas is one method for increasing the quantity ozone delivered per unit of time. For a given ozone gas input concentration, it has been observed that microbubble systems achieve a higher k_La when directly compared with conventional bubble systems (Table 1). With an ozone input concentration that ranged from 10 to 233 mg L^{-1}, the range of reported k_La values was between 0.023 – 1.5 min^{-1} for microbubbles and 0.0055 – 1.11 min^{-1} for conventional bubbles. The maximum observed enhancement was 5.2 times with microbubbles (Zhang *et al*., 2018). The minimum observed enhancement was 1.2 times (Liu *et al*., 2010). The average observed enhancement factor was 2.5 ± 1.3 times. While it is apparent that more reliable comparisons are needed, the data shows that for a given ozone concentration, the mass transfer of ozone into water is significantly

higher for microbubbles than when compared to conventional bubbles. The main driver for this improvement is linked to the increased surface area available for gas transfer.

The effect of ozone input dose on k_La has also been studied for microbubbles without comparison to conventional bubbles. Zhang *et al*. (2013) found that increasing the ozone input dose from 40 to 140 mg L^{-1} resulted in an increase in k_La from 0.18 to 0.32 min^{-1}. Similarly, Khuntia *et al*. (2013) found that increasing the ozone input dose from 329 to 1000 mg L^{-1} resulted in an increase in k_La from 0.11 to 0.17 min^{-1}. In contrast, when the ozone input concentration was increased from 30 to 75 mg L^{-1}, Huang *et al*. (2019) observed no increase in k_La which remained at 0.73 min^{-1}. Where an increase has been seen, the authors have explained this as a function of increasing ozone input concentration. Since there is a higher concentration of ozone in the input gas, both the concentration and rate of ozonation increased (Khuntia *et al*., 2013). An alternative view is that the steady-state concentration should increase linearly with increasing ozone input concentration but k_La should remain almost constant irrespective of input dose since (Al-Abduly *et al*., 2014). Further data is needed to confirm whether these mechanisms hold true for all circumstances where microbubbles are used.

Table 1. Enhancement factor of microbubble k_La against conventional bubble k_La for a fixed input concentration.

Input Concentration / mg L^{-1}	**Microbubble k_La / min^{-1}**	**Conventional k_La / min^{-1}**	**Enhancement Factor**	**Reference**
90	0.23	0.11	2.09	Sun *et al*. (2020)
20	0.54	0.35	1.54	Wu *et al*. (2019)
25	1.36	1.11	1.23	Nam *et al*. (2019)
233	0.023	0.0055	4.18	Gao *et al*. (2019)
47.5	0.23	0.044	5.23	Zhang *et al*. (2018)
12	0.38	0.17	2.24	Zheng *et al*. (2015)
36	0.3	0.2	1.50	Liu *et al*. (2010)
132	0.26	0.14	1.86	Chu *et al*. (2007)
10	1.5	0.54	2.78	Shin *et al*. (1999)

2.4. *Effect of Superficial Gas Velocity on k_La*

The gas flow rate determines the total amount of ozone that is delivered per unit time and can impact bubble size and number concentration. It is conventional to express the flow rate as a superficial gas velocity to account for variations in reactor sizes. The superficial gas velocity is the apparent speed that a gas moves through the liquid (Equation 6) as a function of gas flow rate (Muroyama *et al*., 2013):

$$u_g = \frac{Q_g}{A} \quad (6)$$

Where u_g is superficial gas velocity (m s^{-1}), Q_g is gas flow rate (m^3 s^{-1}) and A is cross sectional area (m^2). Typical superficial gas velocities in full scale plants are 0.26 – 0.87 m min^{-1} (Secula *et al*., 2013) and this compares to experimental systems which vary between 0.0038 and 0.26 m min^{-1}.

For a given superficial gas velocity, several comparisons of microbubbles and conventional bubbles are available (Figure 6). It has been found that the average k_La enhancement factor is 2.3 ± 1.3 where the minimum enhancement was 1.2 times (Nam *et al*., 2019) and the maximum was 5.2 times (Zhang *et al*., 2018). Studies that have looked at the effect of superficial gas velocity for microbubble k_La have been undertaken but have not been directly compared with results from conventional bubbles. Li and Tsuge (2006) observed a linear increase in k_La from 0.12 to 0.44 min^{-1} when the superficial gas velocity was increased from 8 x 10^{-3} to 4.8 x 10^{-2} m min^{-1}. Huang *et al*. (2019) extended the range to higher superficial gas velocities of 6.5 x 10^{-2} to 0.26 m min^{-1} and saw an increase of k_La from 0.64 to 0.79 min^{-1} for a microbubble system using 20 – 30 µm bubbles in deionized water.

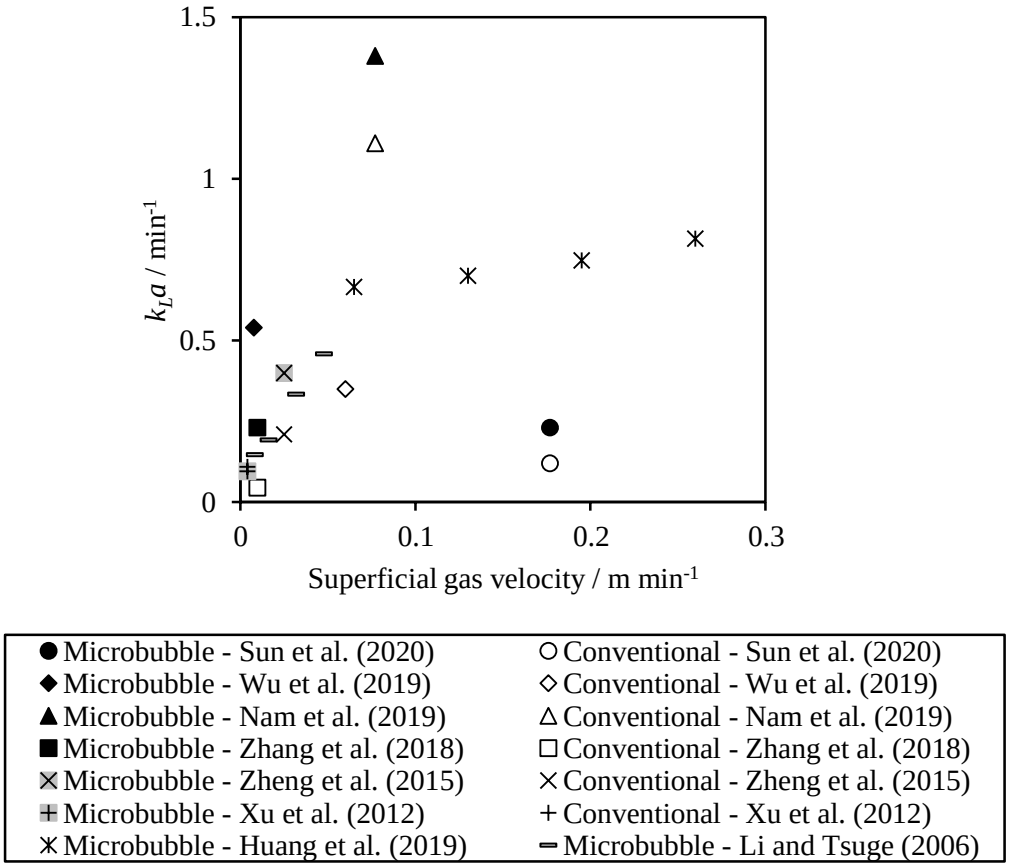

Figure 6. k_La vs. superficial gas velocity for microbubble and conventional bubble ozonation.

2.5. *Gas Utilization Efficiency*

Gas utilization efficiency relates to how much of the supplied gas is transferred into the liquid and is calculated as (Tizaoui and Zhang, 2010; Zhang *et al*., 2013):

$$U = 100\,\frac{C_{in} - C_{out}}{C_{in}} \qquad (7)$$

Where U is the gas utilization efficiency (%), C_{in} is the inlet ozone concentration (mg L^{-1}) and C_{out} is the ozone off-gas concentration (mg L^{-1}).

Since the percentage of ozone by weight in the output gas for an air fed ozone generator is typically around 6 % (Achar *et al*., 2020), optimization of gas transfer is critical to minimizing energy and associated operating costs. The ability to increase gas utilization efficiency is one of the most frequently mentioned favorable properties of microbubbles. Despite this, gas utilization efficiency is one of the least frequently reported measurements and there is a paucity of direct comparisons between microbubbles and conventional bubbles (Table 2). The studies that have been reported confirm the expected enhancement when using microbubbles. For instance, Zhang *et al*. (2018) reported a gas utilization efficiency of 96% for ~51 µm bubbles compared with 60% for conventional bubbles (size not reported) in a shallow 32 cm deep tank with deionized water. A similar enhancement of 85% compared with 48% was also reported by Zheng *et al*. (2015) who compared < 45 µm bubbles with a conventional system in "clean" water using a 1.2 m deep tank. Similarly, gas utilization efficiency was observed to improve from 72 – 79% to 99.0 – 99.5 % in another study that compared conventional bubbles (size not reported) with 50 µm microbubbles (Liu *et al*., 2010). Tank depth was not reported in this work.

Table 2. Gas utilisation efficiencies for microbubble ozonation.

Column Height / m	**Gas Utilisation Efficiency / %**		**Gas Utilisation Efficiency / % m^{-1}**		**Reference**
	MB	**CB**	**MB**	**CB**	
Not reported	92.2 - 99.5	NR	NR	NR	Liu *et al*. (2018)
0.32	96	60	300	187.5	Zhang *et al*. (2018)
1.2	85	48	70.8	40	Zheng *et al*. (2015)
Not reported	83 - 95	NR	NR	NR	Zhang *et al*. (2013)
Not reported	99 - 99.5	72 - 79	NR	NR	Liu *et al*. (2010)

The overall view is that microbubbles have great potential for application with respect to gas utilization efficiency. However, an observation that has consistently arisen from ozonation studies that have compared microbubbles with conventional bubbles has been the use of relatively shallow columns. The maximum column height used was 1.2 m, with some used as low as 0.3 m (Table 3). However, as has been noted, gas transfer tanks are typically much deeper, typically >3m (DeMoyer *et al*., 2001). This tank depth allows sufficient residence time of conventional bubbles, which rise through the water at much faster rates than small bubbles. As a consequence, the use of shallow column heights biases the results in favor of the microbubble systems due to the differences in residence time as a function of bubble size. To illustrate, the residence time for a 50 µm and 2 mm bubble has been calculated for the different sized column heights used in experiments reported in the literature (Table 3). Residence time for the larger bubble was between 0.12 and 0.66 s compared to 197 to 1053 s for the microbubble. To date, there has been no work reported that considers equivalent reactor volume normalized for bubble residence time. For instance, the impact of the height required to transfer 50% of the contents of a bubble has been calculated as a function of bubble size (Figure 7). In the case of a 50 µm bubble, 50 % of its contents can be transferred in less than 2 m of liquid. For a 7 m deep tank, bubbles must be no larger than approximately 200 µm to ensure 50 % utilization (Mueller and Boyle, 2002). If a typical 2 mm bubble is used, water depths exceeding 9 m would be required. While there is compelling evidence for enhanced gas utilization when using microbubbles, it is clear that better experimental comparisons are required that take into account bubble residence times in the reactor to determine whether reactor volume as well as tank depth can also be reduced when using microbubbles.

Table 3. Reported water heights used in microbubble and conventional bubble comparison experiments.

Column Height / cm	Bubble Residence Time / s			Reference
	50 µm Diameter	2 mm Diameter	Difference	
30 (Microbubble) 60 (Conventional)	197	0.25	196.75	Wu *et al*. (2019)
160	1053	0.66	1052.34	Nam *et al*. (2019)
30	197	0.12	196.88	Azuma *et al*. (2019)
80	526	0.33	525.67	Hu and Xia (2018)
31.8	209	0.13	208.87	Zhang *et al*. (2018)
120	790	0.49	789.51	Zheng *et al*. (2015)
60	395	0.25	394.75	Xu *et al*. (2012)
120	789	0.49	788.51	Li and Tsuge (2006)
30	197	0.12	196.88	Shin *et al*. (1999)

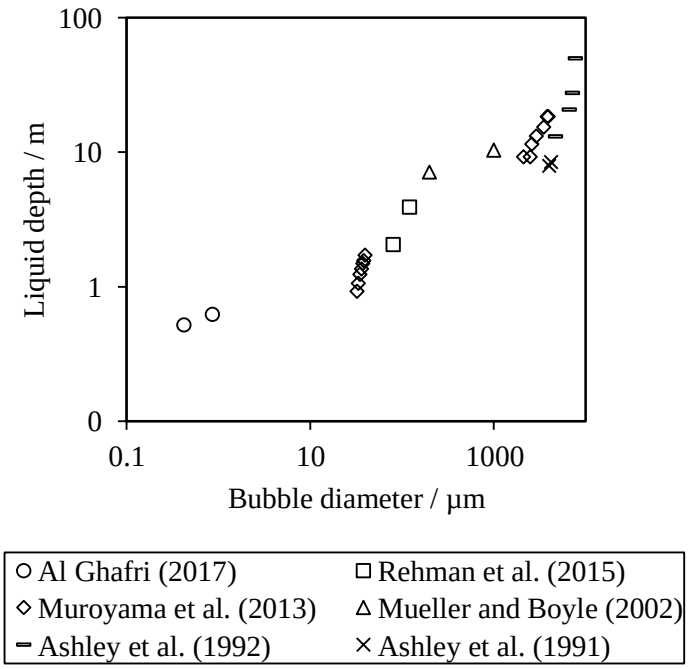

Figure 7. Liquid depth required for 50 % diffusion to occur for a given bubble diameter.

2.6. *Rate of Ozone Self-Decomposition, k_D*

When ozone is dissolved in water, it undergoes a complex self-decomposition reaction chain. The current generally accepted decomposition model is based around the peroxone process (Equations 8 – 14) (Bezbarua and Reckhow, 2004; Fábián, 2006; Ignatiev *et al*., 2008). The hydroxide ion is an initiator in the self-decomposition of ozone (Equation 8) and the hydroxyl radical, a non-selective, highly oxidizing species, is a desirable decomposition product which can react with compounds that are not readily oxidized by molecular ozone (Equation 14). Ozone is not only consumed during decomposition; it is also regenerated. This means that the rate of ozone self-decomposition cannot be inferred from the rate of oxygen and electron transfer but must incorporate the regeneration step (Equation 14) (Gardoni *et al*., 2012).

$O_3 + OH^- \rightarrow O_2 + HO_2^-$ $\quad k_3 = 70\ M^{-1}\ s^{-1}$ (8)

$O_3 + HO_2^- \rightarrow O_3^{\bullet -} + HO_2^{\bullet}$ $\quad k_4 = 2.8 \times 10^6\ M^{-1}\ s^{-1}$ (9)

$HO_2^{\bullet} \leftrightarrow O_2^{\bullet -} + H^+$ $\quad k_5 = 3.2 \times 10^5\ s^{-1}$ $\quad k_{-5} = 2.0 \times 10^{10}\ M^{-1}\ s^{-1}$ (10)

$O_2^{\bullet -} + O_3 \rightarrow O_3^{\bullet -} + O_2$ $\quad k_6 = 3.2 \times 10^5\ s^{-1}$ (11)

$O_3^{\bullet -} + H^+ \leftrightarrow HO_3^{\bullet}$ $\quad k_7 = 5.2 \times 10^{10}\ M^{-1}\ s^{-1}$ $\quad k_{-7} = 3.3 \times 10^2\ s^{-1}$ (12)

$HO_3^{\bullet} \rightarrow OH^{\bullet} + O_2$ $\quad k_8 = 1.1 \times 10^5\ s^{-1}$ (13)

$O_3^{\bullet -} + OH^{\bullet} \rightarrow O_3 + OH^-$ $\quad k_9 = 2.5 \times 10^9\ M^{-1}\ s^{-1}$ (14)

A second reaction chain involving HO_4^- and HO_5^- intermediates has since been proposed (Equations 15 – 24) (Sein *et al*., 2007; von Sonntag, 2008). However, the HO_5^- intermediate has not been observed experimentally (Gardoni *et al*., 2012).

$O_3 + OH^- \rightarrow HO_4^-$ $\quad k_{10} = k_3$ (15)

412 $HO_4^- \leftrightarrow HO_2^\bullet + O_2^{\bullet-}$ $k_{11} \approx 10^7$ s^{-1} $k_{-11} = 5.0 \times 10^9$ M^{-1} s^{-1} (16)

413 $HO_2^\bullet + O_2^{\bullet-} \rightarrow HO_2^- + O_2$ $k_{12} = 10^8$ M^{-1} s^{-1} (17)

414 $O_3 + HO_2^- \rightarrow HO_5^-$ $k_{13} = k_4$ (18)

415 $HO_5^- \leftrightarrow HO_2^\bullet + O_3^{\bullet-}$ $k_{14} \approx 10^7$ s^{-1} $k_{-14} = 5.0 \times 10^9$ M^{-1} s^{-1} (19)

416 $HO_2^\bullet \leftrightarrow O_2^{\bullet-} + H^+$ $k_{15} = k_5$ $k_{-15} = k_{-5}$ (20)

417 $O_2^{\bullet-} + O_3 \rightarrow O_3^{\bullet-} + O_2$ $k_{16} = k_6$ (21)

418 $O_3^{\bullet-} \leftrightarrow O^{\bullet-} + O_2$ $k_{17} = 1.94 \times 10^3$ s^{-1} $k_{-17} = 3.5 \times 10^9$ M^{-1} s^{-1} (22)

419 $O^{\bullet-} + H_2O \leftrightarrow OH^\bullet + OH^-$ $k_{18} = 9.6 \times 10^7$ s^{-1} $k_{-18} = 1.2 \times 10^{10}$ M^{-1} s^{-1} (23)

420 $OH^\bullet + O_3 \rightarrow O_2 + HO_2^\bullet$ $k_{19} = 1.0 \times 10^9$ M^{-1} s^{-1} (24)

421

422 As such, there is yet no agreed upon model for the self-decomposition of ozone, despite being
423 studied for 100 years (Gardoni *et al*., 2012). Consensus leans towards the use of first order
424 degradation kinetics (Lòpez-Lòpez *et al*., 2007; Vyong Tkhi *et al*., 2009;), although 1.5 order
425 (Ku *et al*., 1996; Kuo *et al*., 1977) and second order (Ershov and Morozov, 2009; Gurol and
426 Singer, 1982; Kong *et al*., 2003) have also been proposed. Reaction orders that are pH
427 dependent have also been considered (Haruta and Takeyama, 1981; Hsu *et al*., 2002; Morooka
428 *et al*., 1978; Sotelo *et al*., 1987). These differences arise due to the complex reaction chemistry
429 of aqueous ozone and the difficulty of experimental reproducibility (Fábián, 2006).

430 Across the majority of these models, temperature and pressure are considered critical factors
431 because increases in either accelerate self-decomposition (Bín, 2013; Sotelo *et al*., 1987).
432 Several parameters within the water matrix have also been reported to have significant effects
433 on self-decomposition kinetics including alkalinity, hardness, solids, organic matter and metal

ions (Hoigné, 1994). This is because different contaminants, present in trace concentrations (Bín, 2013), can initiate, promote or terminate the self-decomposition reaction chain depending on how the particular contaminant interacts with molecular ozone and its decomposition products. For instance, if the water matrix contains high concentrations of initiators that promote the decomposition of ozone, then indirect ozonation reactions will predominate. Similarly, appreciable concentrations of compounds that terminate the decomposition reaction chain, for example radical scavengers such as tert-butyl alcohol, will result in the domination of direct molecular ozone reactions (Gardoni *et al*., 2012).

The k_D value in conventional bubble ozonation systems has been modelled across the full pH range (Figure 8). In contrast, there have been relatively few attempts to characterize the self-decomposition profile for microbubble systems or compare k_D in microbubble and conventional systems directly. Where the k_D values of microbubble and conventional systems have been compared (Wu *et al*., 2019) it was found that at pH < 7, the k_D values for both systems were almost identical with values of 0.009 min^{-1} at pH 3 and 0.01 min^{-1} at pH 5. The microbubble system showed a slightly higher k_D at pH 7 with a value of 0.031 min^{-1} compared with 0.023 min^{-1} for the conventional system. The difference between the two systems increased further at pH 9 with values of 0.16 and 0.14 min^{-1} for the microbubble and conventional bubble systems, respectively. The increase in k_D is promoted at higher pH when there are more hydroxide ions present in the water since the hydroxide ion initiates the self-decomposition reaction chain (Equations 8, 15). This leads to a higher concentration of hydroxyl radicals since it is a product of self-decomposition and more extensive initiation of the reaction chain will result in higher concentrations of decomposition products (Equations 13, 23). This is the reason why pH elevation is considered as one of the most effective methods for enhancing ozonation processes through increased hydroxyl radical formation (Miklos *et al.*, 2018)

The explanation for the increase in k_D for microbubbles over conventional bubble systems is frequently explained by an increase in hydroxyl radical formation for the microbubble systems as a result of the spontaneous collapse of these smaller bubbles. It has been reported that, since the internal pressure of a bubble is inversely proportional to its spherical diameter, a localized region of high pressure is formed during the collapsing process and forms a hot-spot due to adiabatic compression (Agarwal *et al*., 2011). It has been proposed that this phenomena causes the spontaneous generation of hydroxyl radicals due to pyrolytic decomposition of ions at the gas liquid interface. There is some evidence to suggest that strongly acidic conditions could alter the zeta potential such that bubble collapse is accelerated enough due to increased repulsion of the bubble wall to cause the generation of hydroxyl radicals (Takahashi *et al*., 2007). Another study found that the k_D for microbubble ozonation in deionized water was higher than that seen for conventional bubbles with values of 0.049 min^{-1} and 0.0135 min^{-1} (Zhang *et al*., 2018). Again, the increase in k_D was attributed to the spontaneous generation of hydroxyl radicals upon the collapse of microbubbles. Increased hydroxyl radical formation from bubble collapse in microbubble ozonation has also been reported to increase the degradation rate of pollutants (section 3).

However, it has been argued that the collapse of a microbubble is not strong enough to cause the spontaneous generation of hydroxyl radicals under normal conditions with no external stimulus since this would require localized temperatures in the region of 5000 Kelvin. Such conditions can normally only be achieved when using a stimulus such as ultrasound (Agarwal *et al*., 2011; Takahashi *et al.,* 2007). In most reported cases of reactive oxygen species being formed directly from bubble collapse, these observations relate to small nanobubbles (Liu et al., 2016)

The increased production of hydroxyl radicals in microbubble systems is therefore still under debate and is an area that warrants further investigation. This is particularly the case when

considered alongside other reported k_D values for microbubbles and conventional bubbles that have not been compared directly in the same studies (Figure 8). These values have been aggregated and averaged for both microbubbles and conventional bubbles to provide a comprehensive comparison between the two. The comparison shows that the k_D is, on average, slightly lower for microbubbles than for conventional bubbles, albeit not statistically different. To illustrate, the k_D average value from 6 researchers for microbubbles was 0.026 ± 0.014 min^{-1} at pH 7 (Wu *et al*., 2019; Zhang *et al*., 2018; Jabesa and Ghosh, 2016b; Khuntia *et al*., 2014; Kukuzaki *et al*., 2010). The average k_D value from 9 researchers for conventional bubbles was 0.047 ± 0.038 min^{-1} at pH 7 (Dehouli *et al*., 2010; Gao *et al*., 2005; Ignatiev *et al*., 2008; Lovato *et al*., 2009; Sotelo *et al*., 1987; Uhm *et al*., 2009; Valdes *et al*., 2009; Wu *et al*., 2019; Zhang *et al*., 2018).

The evidence therefore points to the view that the improvements in microbubble performance are more linked to the fact that these small bubbles reside in the bulk liquid and diffuse their contents longer than is seen for conventional bubbles rather than accelerated hydroxyl radical formation from bubble collapse; the latter mechanism only being important for much smaller bubble sizes

	Number of Reports	
pH	**MB**	**CB**
1 - 1.9	-	1
2 - 2.9	-	4
3 - 3.9	1	3
4 - 4.9	-	5
5 - 5.9	3	6
6 - 6.9	1	7
7 - 7.9	6	9
8 - 8.9	-	4
9 - 9.9	3	4
10 - 10.9	-	1
11 - 11.9	-	3
12 - 12.9	-	2
13 - 13.9	-	2
14	-	1

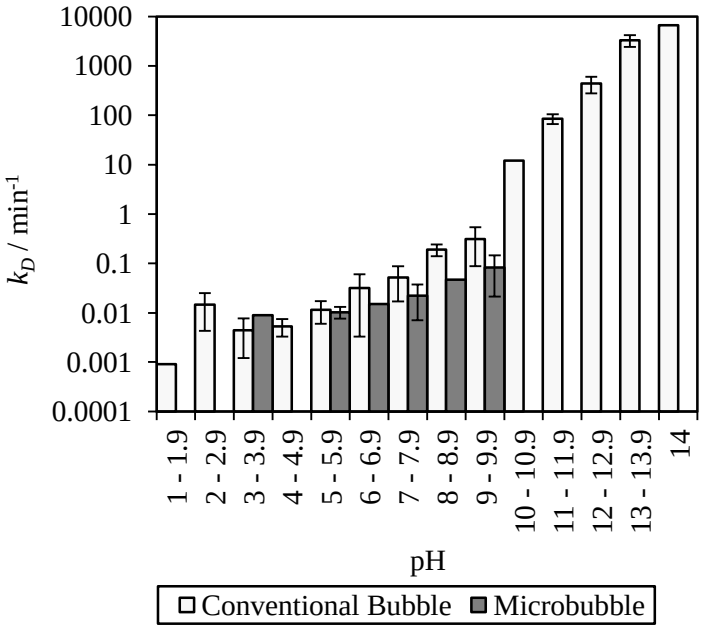

Figure 8. Aggregated k_D values for microbubble (MB) and conventional bubble (CB) ozone self-decomposition with respect to pH.

2.7. *Steady-State Ozone Concentration*

The steady-state ozone concentration is an important process consideration for contactor sizing and design. The aim is to achieve a sufficient ozone residual suitable for treatment, without sending the residual ozone downstream of the contactor. The steady-state ozone concentration is influenced by numerous factors. This includes the gas phase ozone input concentration, gas utilization efficiency, ozone consumption from reactions with contaminants, temperature, pH and the rate of ozone self-decomposition (Lage Filho, 2010). To determine the steady-state condition for a given system, non-steady-state semi-batch tests are conducted until the mass balance reaches equilibrium (Equation 25) (Wu *et al.*, 2019):

$$0 = k_L a(C^* - C_s) + k_D C_s \quad (25)$$

Where C^* is the steady-state equilibrium ozone concentration (mg L^{-1}) and C_s is the steady-state ozone concentration in the bulk liquid (mg L^{-1}). Due to the self-decomposition of ozone, the steady state concentration in the bulk liquid is lower than the ozone concentration at equilibrium (Rischbieter *et al*., 2000). The higher gas utilization efficiency and higher observed rate of volumetric mass transfer means that microbubble systems deliver more ozone at a faster rate into the liquid phase than when compared to conventional bubbles. As a result, and based on previous mass transfer observations, a higher steady-state concentration of dissolved ozone is typically achievable when using microbubbles (Figure 9).

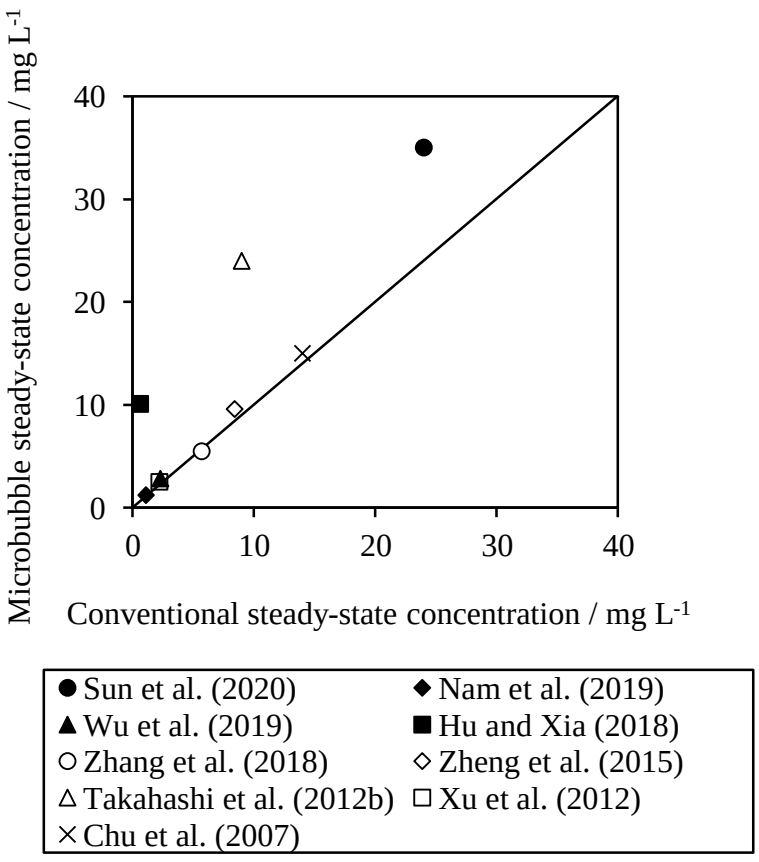

Figure 9. Observed microbubble steady-state ozone concentration vs. observed conventional bubble steady-state concentration in direct comparison experiments.

Wu *et al*. (2019) observed a 1.15 - 1.7 times higher steady state ozone concentration for microbubble ozonation across the pH range 3 – 11 when compared to conventional bubble systems. Steady state concentrations that were 1.1 (Chu *et al*., 2007), 1.15 (Zheng *et al*., 2015), 1.23 (Nam *et al*., 2019) and 2.7 (Takahashi *et al*., 2012b) times higher have also been observed. Zhang *et al*. (2018) did not observe a significant difference between microbubble and conventional bubble steady state concentrations, with reported ozone concentrations of 5.5 and 5.7 mg L^{-1}, respectively. However, in this case, the microbubble system reached the steady state condition considerably faster with k_La values of 0.227 and 0.044 min^{-1}. Hu and Xia (2018) reported a steady state ozone concentration of 10.09 and 0.64 mg L^{-1} with microbubbles and conventional bubbles, respectively, an observed increase of 15.8 times. It was not always clear why some studies reported differences in steady state ozone concentration, while others did not. This was most probably linked to the differences in reactor geometry and depth and the variable experimental set-ups used (see SI 3). In the case of Hu and Xia (2018), the large difference in steady state concentration was thought to driven by the size of the bubbles generated. Hu and Xia (2018) reported the use of “micro-nano” bubbles with a Sauter mean diameter of 247 ± 9 nm, approximately two orders of magnitude smaller than microbubbles used in other studies.

The main difference between microbubbles and conventional bubble systems was the rate at which the steady state was achieved. Where microbubbles and conventional bubbles have been directly compared, the microbubble k_La has been shown to be higher than for the conventional bubble k_La. The implication of a higher achievable steady state concentration for a given ozone input is that the amount of ozone generation required to maintain equivalent treatment is decreased due to the more efficient gas transfer. The following section considers how this translates to degradation of pollutants in water by ozone.

3. Application of Microbubble Ozonation for Degradation of Contaminants

Ozone-based oxidation and disinfection can be broadly categorized into two types of reaction: direct reactions with molecular ozone and indirect radical reactions. Unsaturated organic compounds are typically easily oxidized through direct reactions with molecular ozone (Figure 10). Indirect ozone reactions are much more complex and stem from the decomposition of ozone into hydroxyl radicals. The hydroxyl radical is associated with the non-selective removal of recalcitrant compounds due to its powerful oxidizing capability. Degradation of different contaminant groupings by ozone oxidation delivered by microbubbles and conventional microbubbles are considered in the following sections.

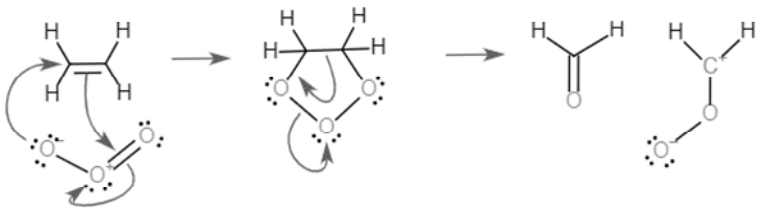

Figure 10. A typical direct ozone reaction with an unsaturated organic molecule.

3.1. *Dyestuff*

Ozone is commonly used for the degradation of dyes (Takahashi *et al*., 2012a) and the use of microbubble systems has been considered as a way of increasing their rate of removal. Comparison of reported studies supports this view, with enhanced reaction rates between 1.1 – 29 times that seen in the comparative conventional system (Figure 11). To illustrate, the rate constant for removal of red 3R dye was increased from 0.061 min^{-1} in the conventional system compared to 0.11 min^{-1} using a ~ 51 µm microbubble in a 0.32 m deep tank (Zhang *et al*., 2018). Similar enhancements have been observed for the treatment of congo red dye from 0.235 min^{-1} with conventional bubbles to 0.385 min^{-1} with microbubbles (Khuntia *et al*., 2016),

587 Reactive black 5 (RB5) dye from 0.092 to 0.16 min^{-1} (Chu *et al*., 2007) and methyl orange
588 from 8.1 x 10^{-3} to 0.24 min^{-1} (Hu and Xia, 2018). Similarly, Takahashi *et al*. (2012a) tested
589 four different dyes (reactive blue, reactive yellow, direct yellow, orange I) and observed that
590 the rate constant was enhanced by 1.1 – 3.1 times when using a microbubble system with a
591 bubble size of 15 – 40 µm in a water depth of 1.2 m.

592

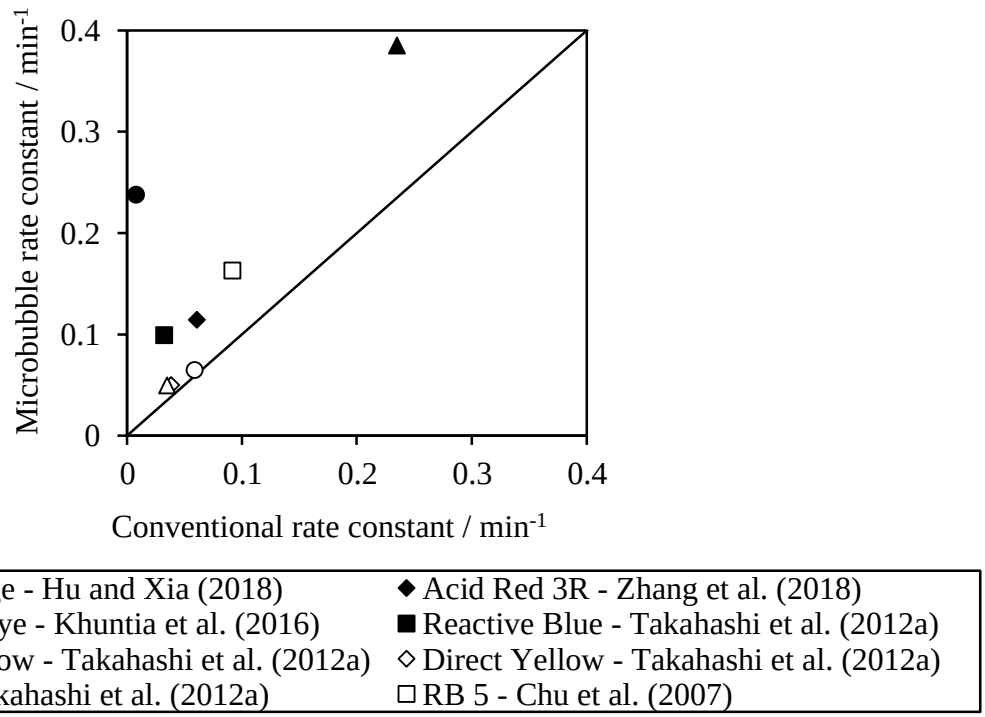

593 **Figure 11.** Rate constants for microbubbles and conventional bubbles for removal of dyestuff
594 in direct comparison experiments.

595 Whilst the rates of degradation were different, the absolute removal of contaminants over the
596 total duration of the experiments were similar for microbubbles and conventional bubbles. This
597 has been seen over a 60 minute exposure experiment using acid red 3R dye (Zhang *et al*., 2018),
598 for reactive blue and orange I dyes over a 120-minute experiment (Takahashi *et al*., 2012a),
599 congo red dye over 20 minutes (Khuntia *et al*., 2012) and for RB5 dye during a 120-minute
600 experiment (Chu *et al*., 2007). Slight differences were observed when treating reactive yellow

and direct yellow dyes in 2 m deep reactor columns. For conventional ozonation, 94 and 90 % removal was observed for reactive yellow and direct yellow dyes after 90 – 120 minutes. This was in contrast to 95 and 98 % respectively for the microbubble ozonation system in a (Takahashi *et al.*, 2012a).

More significant differences have been reported in an experiment over a shorter duration, treating methyl orange in a 0.8 m tank for 30 minutes (Hu and Xia, 2018). The conventional system achieved only 15% removal compared to 100 % for the microbubble equivalent. It was posited that this was due to the high concentration of dissolved ozone that could be delivered by the microbubble system which reached a maximum of 10 mg L^{-1} whereas the conventional system achieved only 0.64 mg L^{-1}.

3.2. *Pharmaceuticals*

The removal of pharmaceuticals with ozone using microbubble and conventional systems reveal a broader range of impacts, but with the majority of cases showing an improvement when using microbubbles (Figure 12). For instance, Azuma *et al.* (2019) investigated the removal of 39 pharmaceuticals in a 5-minute test using a 0.3 m deep tank. The majority of the compounds were considered to react relatively well with ozone and resulted in more than 99 % removal irrespective of the bubble size used. In contrast, eleven pharmaceuticals showed significantly enhanced removal with microbubble ozonation. These compounds were not easily removed by ozonation. This offers evidence of the potential to extend the range of treatable compounds with ozone by using microbubble delivery systems. These experiments were normalized for input dose over a fixed time period so it can be inferred that the microbubble systems delivered a higher effective dose of ozone. For these experiments, the ozone input concentration was 6.5 mg L^{-1} with a flow rate of 0.018 m^3 hr^{-1} corresponding to a feed rate of

1.0 mg L^{-1} min^{-1}. The calculation of an effective dose was not possible due to the lack of data on gas utilization and dissolved ozone concentration. However, based on ozone consumption there was 2.2 times more ozone consumed with the microbubble system after 5 minutes when compared to the conventional system. This reinforces the view that the explanatory reason for the microbubble improvements is primarily related to the increased in the effective ozone dose supplied. Three further pharmaceuticals (atenolol, ethinylestradiol and ibuprofen) were investigated by Lee *et al*. (2019) and it was found a 1.3 – 2.5 times improvement in the total removal after 5 minutes of ozonation with microbubble ozonation compared with the conventional system.

Whilst the overall removal is important, the rate of degradation should also be considered as it gives a more explicit comparison of the performance differences between microbubbles and conventional bubbles. A faster rate of degradation was observed for 35 of the 39 pharmaceuticals for the microbubble system. The range of removal enhancements was between 1.05 – 104 times, with a median of 2.4, for the microbubble system over the conventional bubbles (Azuma *et al*., 2019). The explanation for these observations was consistent with an increase in the effective ozone dose applied in the microbubble reactor, which in turn led to higher ozone consumption and oxidation. It should be noted that these experiments were performed in a shallow reactor (0.3 m) that would provide much longer residence times for the microbubbles, giving them a longer time period over which to discharge their contents when compared to the conventional bubbles.

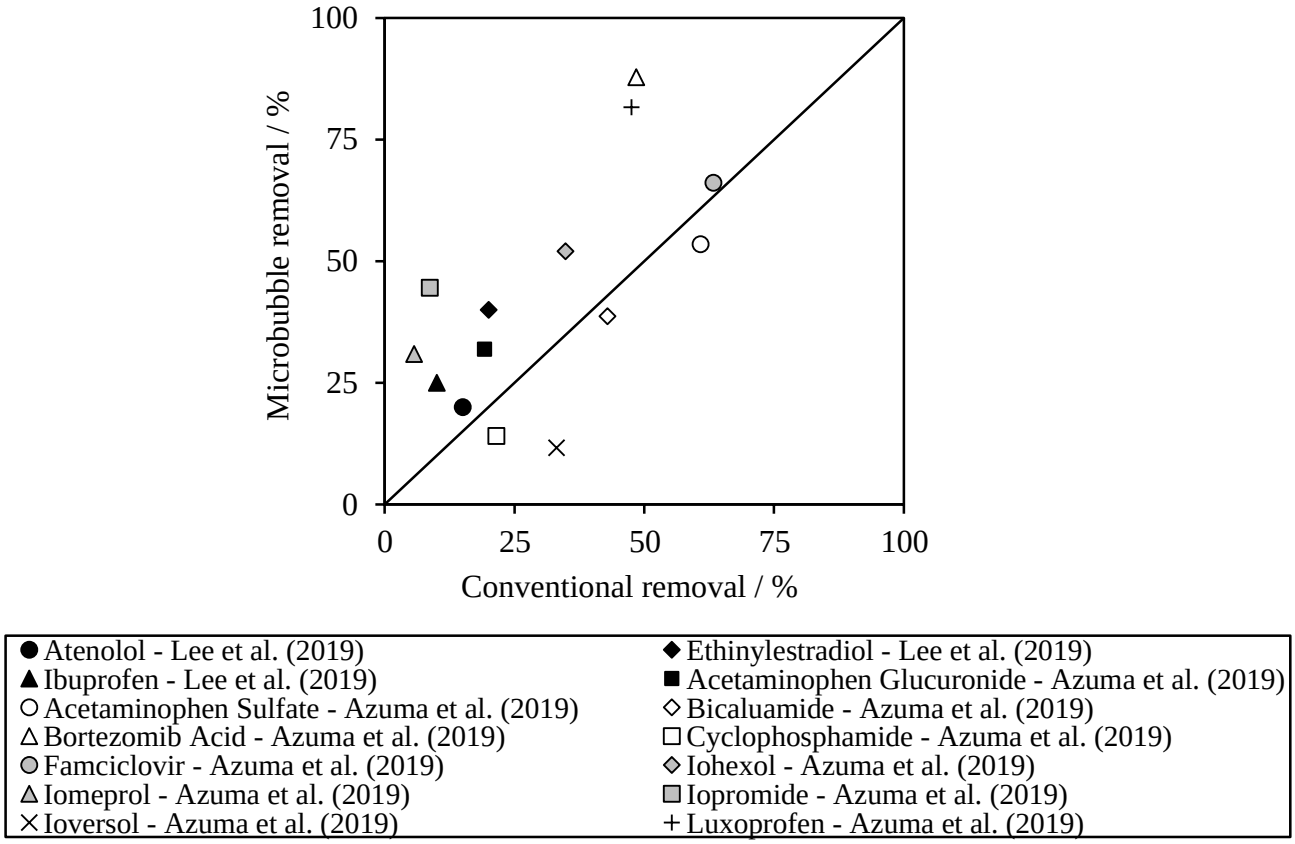

Figure 12. Percentage removal of pharmaceutical chemicals for microbubble and conventional bubbles in direct comparison experiments.

3.3. *Other Organic Compounds*

Microbubble ozonation has been shown to significantly enhance the rate of degradation of a range of other organic compounds (Figure 13). For example, the switch from conventional bubble to microbubble ozonation significantly improved the rate of degradation of p-nitrophenol, with the rate constant increasing from 0.015 to 0.16 min^{-1} (Cheng *et al.*, 2019), nitrobenzene from 0.032 to 0.10 min^{-1} (Wu *et al.*, 2019) and the heterocyclic compound 1,4-

dioxane with an increase from 0.001 to 0.0025 min^{-1} (Xu *et al.*, 2012). For other compounds, a more modest enhancement has been observed such as for phenol with an enhancement from 0.072 to 0.30 min^{-1} based on a 20 – 50 μm microbubble system with a water depth of 0.3 m (Wu *et al.*, 2019).

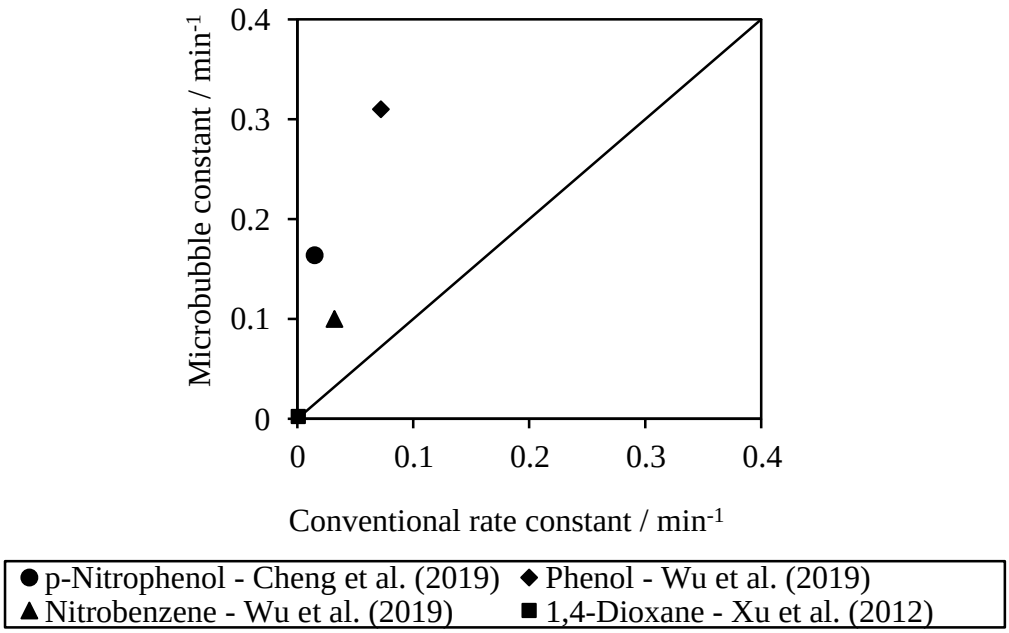

Figure 13. Rate constants for microbubbles and conventional bubbles for removal of a range of organic compounds where they have been directly compared.

The pH of the water has been established to be critical on the rate of compound degradation as the rate of ozone self-decomposition and the generation of hydroxyl radicals are both heavily dependent upon pH. For instance, Wu *et al.* (2019) tested the effectiveness of microbubble ozonation of phenol and nitrobenzene at different pH values (Figure 14). Phenol is a compound that is readily degraded in the presence of both molecular ozone and hydroxyl radicals. It is

reported to have a reaction rate constant with molecular ozone of 1.8 x 10^5 L mol^{-1} s^{-1} (Joshi and Shambaugh, 1982) compared with 6.6 x 10^9 L mol^{-1} s^{-1} for hydroxyl radicals (Buxton *et al.*, 1988). Nitrobenzene is a compound that has a very low reactivity with molecular ozone, with a rate constant of 9 x 10^{-2} L mol^{-1} s^{-1} (Hoigné and Bader, 1983). This is negligible compared to its reaction rate with the hydroxyl radical, reported to be 3.2 ± 0.4 L mol^{-1} s^{-1} (Beltran, 2004; Neta and Dorfman, 1968). Thus, the extent of degradation of nitrobenzene gives an indirect indication of hydroxyl radical production.

The degradation rate of both compounds increased with increasing pH (Wu *et al.*, 2019). For example, the degradation rate constant for the microbubble ozonation of phenol increased from 0.16 min^{-1} at pH 3 to 0.31 min^{-1} at pH 7 to 0.43 min^{-1} at pH 11. The rate constants were lower for the conventional bubbles, but increased from 0.037 min^{-1} at pH 3 to 0.072 min^{-1} at pH 7 and 0.24 min^{-1} at pH 11. For nitrobenzene, the rate constants were less than those seen for phenol but increased with an increase in pH for both systems. To illustrate, the degradation rate constant increased from 0.014 min^{-1} at pH 3 to 0.032 min^{-1} at pH 7 and to 0.061 min^{-1} at pH 11 for the conventional systems. Higher rate constants were seen for the microbubble system which increased with pH from 0.037 min^{-1} at pH 3 to 0.10 min^{-1} at pH 7 and to 0.16 min^{-1} at pH 11. These results are consistent with the increase in hydroxyl radical formation with increasing pH as a result of the self-decomposition of ozone (Section 2.6).

In some cases, the reported rates of removal with microbubble ozonation has not followed the expected increase with pH. For example, Khuntia *et al.* (2016) reported that an increase in pH from 3 to 7 to 9 resulted in a consistent increase in the rate of colour removal of congo red dye with conventional bubble ozonation from 0.21 to 0.235 to 0.255 min^{-1}. The microbubble system, however, followed a different pattern in which reaction kinetics were similar at pH 3, 7 and 9, resulting in rate constants of 0.40, 0.385 and 0.41 min^{-1}, respectively. In this case, the rate constants for degradation of this compound were comparatively high, suggesting that the

compound was efficiently degraded by ozone. As there was little sensitivity to pH, molecular ozone was likely to be responsible for breaking down the dye molecule and hence the removal of color from the water.

The results show that in most comparisons, microbubble processes have faster reaction kinetics than seen for conventional bubbles for a range of contaminants and micropollutants. The pH of the reaction is important for a range of compounds, with higher pH increasing the reaction rate, a result consistent for both conventional bubble and microbubble ozonation. The degree of improvement is dependent on the sensitivity of the compound to degradation by either ozone or hydroxyl radicals.

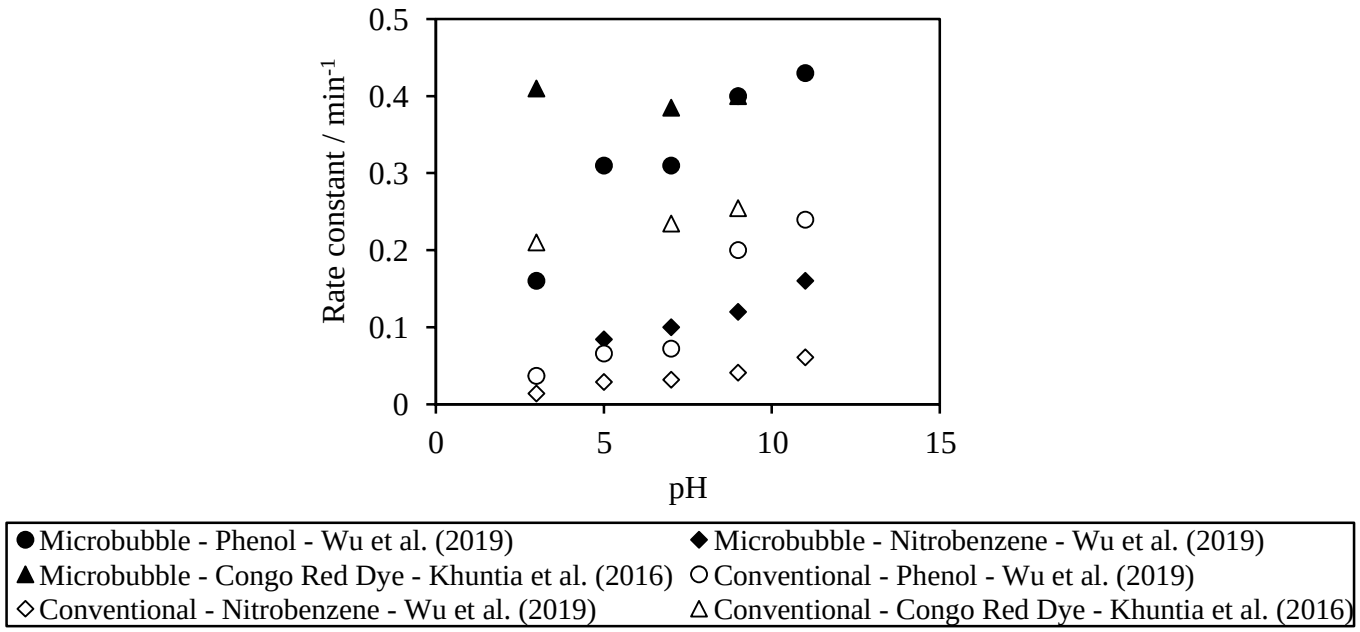

Figure 14. The impact of increasing pH on the rate constant for removal of various compounds by ozonation using microbubbles and conventional bubbles.

4. Challenges and Future Prospects of Microbubble Ozonation

The advantages of enhanced ozone mass transfer for microbubble systems have been shown to be predominantly related to the increase in specific surface area and the increased bubble residence time within the water column. The review of comparative studies has shown that microbubbles afford opportunities for improving existing ozonation systems. The following section discusses how microbubbles could be practically implemented by considering: 1) microbubble generation methods; 2) reactor configurations and 3) further challenges to address.

4.1 Microbubble generation methods

The main challenges associated with the application of microbubble generators in water treatment are around scale-up and process design. At present the vast majority of work, particularly for low-powered microbubble generators, has been carried out at laboratory and pilot scale. Those systems that have been developed for full-scale implementation can treat flows around 1 megalitre per day (MLD) with a power requirement under 1 kWh m^{-3}. As such, commercially available microbubble generators would only be able to treat relatively modest flows. However, advancements in generation systems are making the application more feasible for larger systems.

There are several different methods for generating microbubbles and their modes of action has been comprehensively reviewed previously (Temesgen et al., 2019; Parmar and Majumder, 2013; Khuntia *et al*., 2012). All of these generators produce bubbles based on a reduction in pressure caused by surface tension and a change in energy causing cavitation and bubble formation (Temesgen et al., 2019). Cavitation can be achieved hydrodynamically or through the application of an acoustic field. The hydrodynamic approach is the most widely used

732 method due to a more favourable energy balance and is the focus of the discussion here. The
733 most common types of hydrodynamic microbubble generator are ones that use turbulent flow,
734 mechanical shear, pressurized dissolution and forced bubble detachment (Table 4).

735 Specifically for ozone applications, mechanical shear and pressurized dissolution types of
736 system have been used, often in combination with one another. Mechanical shear microbubble
737 generators utilise some form of rotating and pumping device, using centrifugal pumps (da Silva
738 Henauth *et al.*, 2016), turbine pumps (Yao *et al.*, 2016) or external mixing (Li *et al.*, 2016).
739 These systems physically shear the injected gas into microbubbles. In some cases, automatic
740 gas suction is achievable through the introduction of a pressure from a rapidly rotating impeller,
741 but such systems are often used in conjunction with a gas supply (Wu *et al.*, 2019). There is
742 currently little published evidence of large scale application for ozonation using these types of
743 microbubble generator, with the highest reported liquid flow rate of 4.5 m^3 hr^{-1} (Nam *et al.*,
744 2019). These types of microbubble generator are often limited by their capacity for gas flow,
745 which is often only a small percentage of the liquid flow capacity. The highest reported gas
746 flow rate for ozonation was 0.25 m^3 hr^{-1} with a liquid flow rate of 2.4 m^3 hr^{-1} (Takahashi *et al.*,
747 2012a). However, these types of microbubble generators have potential at larger scales, as
748 commercial units are available for dissolved air flotation applications for liquid flow capacities
749 of up to 58 m^3 hr^{-1} and a gas flow capacity of 4.6 m^3 hr^{-1} with a power consumption of 0.52
750 kWh m^{-3} (www.nikunijapan.com). The limiting factors for scale up of these types of
751 microbubble generators is that they require a constant liquid flow, require some level of
752 contactor redesign and require significant power input. In the case of ozonation, preferable
753 application may be to consider dosing ozone into a smaller side-stream flow prior to mixing
754 the concentrated liquid into a larger main flow.

755 The turbulent flow microbubble generator operates by placing a restriction in a pipe of flowing
756 liquid. As the liquid passes through the restriction, the velocity of the flowing liquid increases

and causes a pressure drop to below atmospheric pressure in the region immediately after the restriction. A series of holes allow for the automatic suction of gas. Common types of turbulent flow microbubble generators include the spherical body (Budhijanto *et al*., 2015; Deendarlianto *et al*., 2015; Kawahara *et al*., 2009; Sadatomi *et al*., 2005; Sadatomi *et al*., 2007), orifice (Sadatomi *et al*., 2012), Venturi (Baylar *et al*., 2007; Baylar *et al*., 2010; Rahman *et al*., 2014; Huang *et al*., 2018; Majid *et al*., 2018) and swirling flow (Terasaka *et al*., 2011; Li *et al*., 2013a; Li *et al*., 2013b; Levitsky *et al*., 2016; Yamashita *et al*., 2017; Hu and Xia, 2018; Xu *et al*., 2018). The advantage of these types of microbubble generator is that they have no moving parts and require no power. These systems are somewhat similar to a conventional diffuser, although they require a constant liquid flow in order to operate optimally. The turbulent flow-microbubble generators are scalable, with reported liquid flow rates of up to 30 m^3 hr^{-1} (Sun *et al*., 2017). Commercial Venturi systems are already available for ozonation and typically operated by dosing a high ozone concentration into a side stream flow before being mixed back with the main flow, enabling application in large scale municipal treatment plants.

One of the most novel types of microbubble generator is the fluidic oscillator. This type of generator has a unique mode of operation in which the gas flow oscillates through a specially designed channel which causes the premature detachment of bubbles at the diffuser pores. The research studies undertaken to date with this type of technology have all been associated with small scale trials using gas flow rates of 0.06 m^3 hr^{-1}. However, commercial processes for aeration of wastewater have been developed treating flows of 40 m^3/hr and above (http://perlemax.com/downloads/WW_DZFO_info.pdf). The fluidic oscillator has been demonstrated to be superior to a standalone diffuser, primarily in aeration and flotation applications (Hanotu *et al*., 2012; Hanotu *et al*., 2014; Abdulrazzaq *et al*., 2015; Al-Mashhadani *et al*., 2015; Hanotu *et al*., 2016; Hanotu *et al*., 2017). Although no published examples of fluidic oscillation for ozonation were identified, the advantage of this type of

782 microbubble generator being that it would act effectively as an in-line addition to existing
783 diffusers and would not require extensive redesign of ozone contactors (Zimmerman *et al.*,
784 2011b).

785 The key consideration for the more wide scale application of microbubble generators is the
786 operational limitation associated with gas and liquid flows. Unlike conventional diffusers, the
787 majority of microbubble generators require a liquid flow. Particularly for the generators that
788 use automatic gas suction or pumping, a constant velocity of liquid passing through the
789 generator is therefore important. In addition, for these types of generator, the gas flow rate is
790 also dependent on water depth (Sadatomi *et al.*, 2012), flow rate (Sadatomi *et al.*, 2005),
791 velocity (Sadatomi *et al.*, 2007), number, size and location of drilled holes (Sadatomi *et al.*,
792 2005) and the size of the restriction. It has also been shown that the diameter of the resulting
793 microbubbles is heavily influenced by the gas and liquid flow rates. Majid *et al.* (2018)
794 observed an increase in bubble diameter from 700µm to 1250µm when gas flow rate was
795 increased from 0.012 to 0.066 m^3 hr^{-1}. However, a decrease in diameter from 700µm to
796 400µm was observed when the liquid flow rate was increased from 1.8 to 4.8 L min^{-1}. It was
797 also noted that increasing gas flow rate decreased the k_La. As such, these factors need to be
798 considered as the capacity of microbubbles systems improves. In WTWs, where the flow is
799 variable, maintaining a constant flow and velocity of water through the generator will
800 becomes an operational challenge. Often the maximum achievable gas flow rate is linked to
801 the liquid flow rate of the generator and it appears that many types of microbubble generator
802 are limited in their ability to significantly adjust gas flow rate. These features mean that the
803 most likely application of microbubbles may be to dissolve ozone into a side stream prior to
804 mixing with the main flow.

805

806

807 **Table 4.** Different types of microbubble generators and their operational gas and liquid flow rates.

Category	Type	Scale	Gas	Gas Flow Rate / m^3 hr^{-1}	Liquid Flow Rate / m^3 hr^{-1}	Reference
Turbulent Flow	Spherical body	Industrial	Air	0.01	2.0	Majid *et al*. (2016)
		Lab	Air	0.04	2.0	Deendarlianto *et al*. (2015)
		Lab	Air	0.05	0.2	Budhijanto *et al*. (2015)
		Lab	Air	0.20	2.2	Kawahara *et al*. (2009)
		Lab	Air	0.51	3.7	Sadatomi *et al*. (2007)
		Lab	Air	0.90	2.5	Sadatomi *et al*. (2005)
	Orifice	Lab	Air	0.06	4.8	Juwana *et al*. (2018; 2019)
		Industrial	Air	0.05	16.0	Majid *et al*. (2016)
		Lab	Air	0.05	3.7	Deendarlianto *et al*. (2015)
		Lab	Air	1.08	3.7	Sadatomi *et al*. (2012)
	Swirling flow	Lab	Ozone	0.24	16.2	Hu and Xia (2018)
		Lab	Air	0.53	0.7	Xu *et al*. (2018)
		Lab	Ozone	0.02	Not reported	Zhang *et al*. (2018)
		Lab	Air	Not reported	0.1	Levitsky *et al*. (2016)
		Lab	Air / Ozone	0.06	1.2	Li *et al*. (2006)
		Lab	Ozone	0.06	1.2	Li and Tsuge (2006)
	Venturi	Lab	Air	0.06	4.8	Majid *et al*. (2018)
		Lab	Air	0.06	4.8	Deendarlianto *et al*. (2017)
		Lab	Air	0.12	30.0	Sun *et al*. (2017)
Mechanical Shear	Gas-liquid mixing pump	Lab	Ozone	0.18	Not reported	Cheng *et al*. (2019)
	Shear force generator	Lab	Ozone	0.03	Not reported	Gao *et al*. (2019)
	Gas-liquid mixing pump	Lab	Ozone	0.18	Not reported	Huang *et al*. (2019)
	Shear force generator	Lab	Ozone	0.06	4.5	Nam *et al*. (2019)
	Centrifugal pump	Lab	Ozone	0.03	0.6	Wu *et al*. (2019)

	Gyratory accelerator	Lab	Ozone	0.04	Not reported	Zhang *et al*. (2013)
	Shear force generator	Lab	Ozone	0.24	2.4	Takahashi *et al*. (2012a)
	Shear force generator	Lab	Ozone	0.00	Not reported	Xu *et al*. (2012)
	Gyratory accelerator	Lab	Ozone	0.03	Not reported	Chu *et al*. (2007)
Pressurized Dissolution	Not reported	Lab	Ozone	0.02	Not reported	Azuma *et al*. (2019)
		Lab	Ozone	0.12	Not reported	Liu *et al*. (2018)
		Pilot	Ozone	Not reported	Not reported	Jabesa and Ghosh (2016a)
		Lab	Ozone	Not reported	Not reported	Khuntia *et al*. (2016)
		Lab	Ozone	0.03	Not reported	Zheng *et al*. (2015)
		Lab	Ozone	Not reported	Not reported	Khuntia *et al*. (2013)
		Lab	Ozone	Not reported	Not reported	Liu *et al*. (2010)
Diffuser	0.22 - 0.55 µm device	Lab	Ozone	0.03	Not reported	Sun *et al*. (2020)
Forced Bubble Detachment	Fluidic oscillation	Pilot	Air	Not reported	Not reported	Hanotu *et al*. (2017)
		Lab	Air	Not reported	Not reported	Hanotu *et al*. (2016)
		Lab	Air	0.06	Not reported	Abdulrazzq *et al*. (2015)

4.2 Reactor configuration

With the incorporation of microbubble generators into ozonation, there is the potential for significant changes to reactor configuration which in turn may reduce capital and operational costs in several areas, including chemical consumption, off-gas destruction, ozone generation and plant footprint. As has been demonstrated, the gas utilisation efficiency of ~100% for microbubbles (Chu *et al*., 2007; Chu *et al.*, 2008; Zhang *et al.*, 2018) has the potential to reduce or remove the need for expensive off-gas destruction systems (Zimmerman *et al.*, 2011). The enhanced gas utilization efficiency infers that less ozone is required in order to achieve a target ozone residual. Based on the difference in k_La for direct comparisons of conventional bubbles with microbubbles, it may be possible to reduce reactor volume by between 16 and 81% when using microbubbles (based on the minimum and maximum k_La enhancement seen by Nam *et al.* (2019) and Zhang *et al.* (2018) respectively), while still achieving similar or better residual ozone concentration (Figure 15). As a consequence, a smaller nominal ozone contactor volume when using microbubbles might be feasible when compared to systems develop using conventionally sized bubbles. Given that the capital cost of an ozonation system is typically 65% of the total cost of an ozonation system, significant reductions may therefore be realized through application of microbubbles. These savings need to be considered alongside the capital costs of multiple microbubble generators (costs not available), as well their operation and maintenance costs.

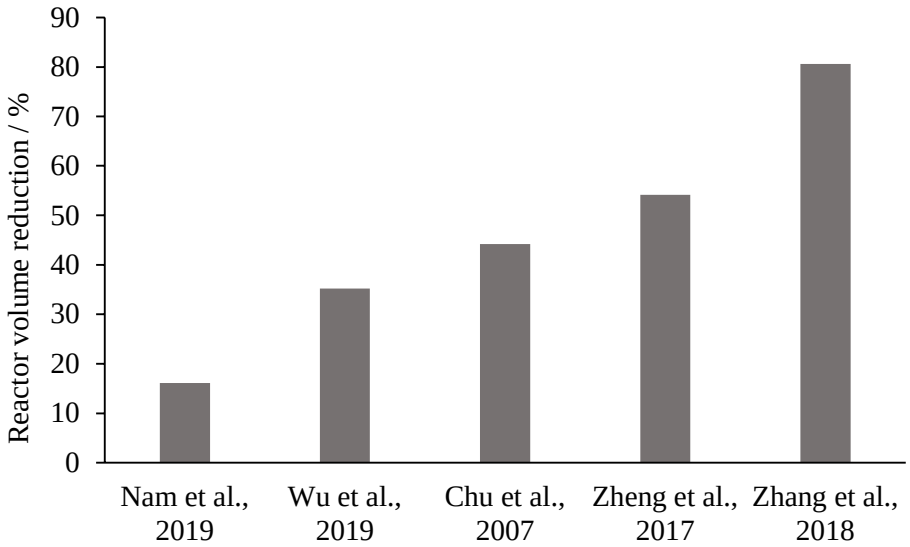

834

835 **Figure 15.** Reactor volume reductions for microbubbles based on k_La difference between
836 experiments carried out for conventional and microbubble systems. Assumption based on
837 removal of fast reacting compounds in mass transfer limited system.

838

839 Whilst the reviewed data presents a strong evidence base for the enhancement that can be
840 delivered through the use of microbubble systems it must be stressed that these data are based
841 on results from laboratory trials. Two approaches for implementation of microbubbles into
842 ozone systems can be considered: in-line or side-stream ozonation (Figure 15). Importantly,
843 the experimental methods employed in most research to date have used relatively shallow water
844 depths, which biases the results in favor of microbubbles in a way that might not be realized in
845 practice. For instance, the high gas utilization efficiencies reported for microbubbles (Table 2)
846 suggest that microbubbles will diffuse the entirety of their contents in less than 1 m of water
847 depth. While this might encourage design of shallower contactors for new ozone installations,
848 there may be more challenging considerations if retrofitting of microbubble ozone systems was
849 being considered. In such cases, the water would require mixing to avoid stratified zones of
850 either high or no dissolved ozone in the reactor. This would have to be achieved through
851 external mixing which will impart additional energy costs which are not generally considered.

However, this also affords an opportunity where ozone mass transfer could be conducted in a side stream unit. The ozonated water in the sidestream would then be recombined into the main flow, maximizing energy utilization and enabling constant flow to the contactor to be easily achieved (Figure 15). This approach would also better align with the limited gas and liquid flow rates achievable with current microbubble generators, enabling treatment of larger flows.

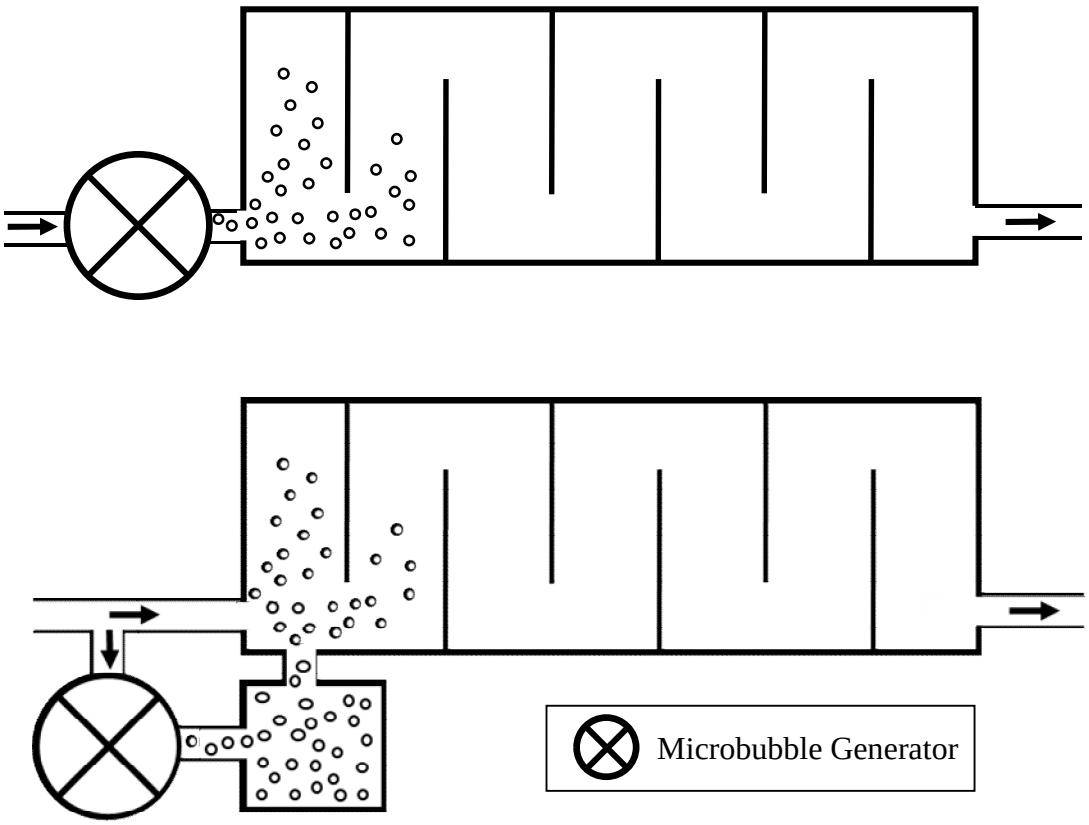

Figure 15. Possible microbubble generator arrangements at full scale where the top figure is in-line and bottom is the side-stream mode.

4.3 Further challenges to address

Given the faster reaction kinetics observed for microbubbles in shallow columns in comparison to conventional bubbles, this might afford opportunities for reduced volumes and contact times in shallower reactors. Accordingly, the impact of water depth on the assessment of the efficacy of microbubble compared to conventional systems requires further investigation. In addition, this would provide clear evidence of the true impact of reducing bubble size on the enhancement of mass transfer and degradation kinetics to enable translation into real systems. This would also provide the framework for a standard approach to testing enabling comparison between different microbubble technologies. To achieve this more consistent and accurate bubble sizing is also required that covers both microbubbles and conventional systems to better refine the comparisons and reactor geometries. This also needs to consider variables that are not usually reported in comparative studies, such as bubble delivery in the water column and the density (concentration) of bubbles.

While the high surface area to volume ratio confers significant mass transfer advantages for microbubbles, this feature may also result in disadvantages when bubble coating is considered. Microbubble systems will be potentially more impacted by material accumulation from surface active compounds than when larger bubbles are used (Parkinson *et al.*, 2008). This is an important aspect to consider given that most of the aforementioned microbubble ozonation studies have investigated contaminant degradation in pure water matrices. Accumulated material at the gas-liquid interface increases surface rigidity, decreases the net buoyancy force by adding weight and adds an additional resistance to mass transfer (Rosso and Stenstrom, 2006). For instance, from the limited studies carried out, surface coating has been associated with a 1.4 reduction in dissolution time (Tanaka *et al.*, 2020) and has been shown to retard the efficacy of degradation of pharmaceuticals (Lee *et al*, 2019). To illustrate, the degradation rate of ethinylestradiol decreased from 0.10 to 0.07 min^{-1} for microbubbles with and without humic

acid surface coatings, corresponding to a 30% retardation of the degradation due to surface coating effects. The equivalent was also seen for conventional bubbles where the coating decreased the degradation rate constant from 0.07 to 0.04 min^{-1}. Similar results were also observed for degradation of ibuprofen and atenolol, with the bigger impact observed for the conventional bubble systems in all cases indicating that the increased surface area reduced the adsorbed layer thickness. However, this is an under explored area as smaller bubbles contain less active reactant material per bubble and so it is suggested that a critical layer thickness to bubble size ratio will exist beyond which all the reactant is utilized in oxidizing the compounds within the surface coating. In such cases, the microbubble systems would exhibit a preferential focus towards hydrophobic compounds and potentially restrict efficacy towards degradation of hydrophilic compounds. The importance of surface coating on microbubble ozonation therefore needs to be established to ensure that the improvements seen in pure water laboratory tests translates across to more complex water matrices containing background organic matter.

There has also been an emergence of studies combining ozone microbubbles with other chemicals and catalyst materials to facilitate enhanced degradation of various contaminants. For example, researchers have combined iron nanoparticles or powdered activated carbon with ozone microbubbles for catalytic treatment of various organic contaminants (Hou *et al.*, 2020; Zhang *et al.*, 2018). Much greater understanding of the role ozone microbubbles play in these processes is required, but there may be potential for the development of systems more comparable with advanced oxidation processes (AOPs) that are currently used for highly recalcitrant pollutants.

5. Conclusions

The adoption of microbubble delivery systems for use with ozone is shown to enhance both the mass transfer rate and the steady state concentration that can be achieved. The enhanced mass transfer rates are observed *ceteris paribus* with specific evidence in relation to input ozone concentration and the superficial gas velocity. Further, the ozone self-decomposition rate appears unaffected by changing bubble size such that the enhanced mass transfer corresponds to an improvement of degradation of target compounds. There was no evidence to show that collapse of microbubbles was a mechanism that contributed to the enhanced performance of the smaller bubbles. The results indicate that more effective treatment of compounds that are currently poorly degraded by conventional ozone systems may be achievable when using microbubbles. However, the evidence is based on experiments utilizing shallow water depth that will positively bias results towards the microbubble systems, which may not be realizable in all practical situations. As such, it is recommended that future work explores the role of water depth along with surface coating to establish a standardized approach for the comparison and selection of microbubble ozone delivery systems for use in water treatment.

Disclosure Statement

No potential conflict of interest is reported by the authors.

Funding

This research is gratefully supported by the Engineering and Physical Sciences Research Council (EPSRC) through their funding of the STREAM Industrial Doctorate Centre (EP/G037094/1) and from the project sponsor Anglian Water.

References

Abdulrazzaq, N., Al-Sabbagh, B., Rees, J., & Zimmerman, W. (2015). Separation of azeotropic mixtures using air microbubbles generated by fluidic oscillation. *Aiche Journal*, *62*(4), 1192-1199. https://doi.org/10.1002/aic.15097

Achar, J., Nam, G., Jung, J., Klammler, H., & Mohamed, M. (2020). Microbubble ozonation of the antioxidant butylated hydroxytoluene: Degradation kinetics and toxicity reduction. *Environmental Research*, *186*, 109496. https://doi.org/10.1016/j.envres.2020.109496

Agarwal, A., Ng, W., & Liu, Y. (2011). Principle and applications of microbubble and nanobubble technology for water treatment. *Chemosphere*, *84*(9), 1175-1180. https://doi.org/10.1016/j.chemosphere.2011.05.054

Akimov, V., Dmitriev, E., & Trushin, A. (2011). Mass transfer in the chemosorption of CO2 in a membrane microbubble apparatus. *Theoretical Foundations of Chemical Engineering*, *45*(6), 811-817. https://doi.org/10.1134/s0040579511060017

Al-Abduly, A., Christensen, P., Harvey, A. & Zahng, K. (2014). Characterization and optimization of an oscillatory baffled reactor (OBR) for ozone-water mass transfer. *Chemical Engineering and Processing: Process Intensification*, *84*, 82-89. https://doi.org/10. 1016/j.cep.2014.03.015

Al-Mashhadani, M., Wilkinson, S., & Zimmerman, W. (2015). Airlift bioreactor for biological applications with microbubble mediated transport processes. *Chemical Engineering Science*, *137*, 243-253. https://doi.org/10.1016/j.ces.2015.06.032

Ashley, K., Hall, K., & Mavinic, D. (1991). Factors influencing oxygen transfer in fine pore diffused aeration. *Water Research*, *25*(12), 1479-1486. https://doi.org/10.1016/0043-1354(91)90178-s

Ashley, K., Mavinik, D., & Hall, K. (1992). Bench-scale study of oxygen transfer in coarse bubble diffused aeration. *Water Research*, *26*(10), 1289-1295. https://doi.org/10.1016/0043-1354(92)90123-l

Azuma, T., Otomo, K., Kunitou, M., Shimizu, M., Hosomaru, K., & Mikata, S. *et al*. (2019). Removal of pharmaceuticals in water by introduction of ozonated microbubbles. *Separation and Purification Technology*, *212*, 483-489. https://doi.org/10.1016/j.seppur.2018.11.059

Baquero-Rodríguez, G., Lara-Borrero, J., Nolasco, D., & Rosso, D. (2019). Review of the Factors Affecting Modeling Oxygen Transfer by Fine-Pore Diffusers in Activated Sludge. *Water Environment Research*, *90*(5), 431-441. https://doi.org/10.1002/wer.1082

Baylar, A., Ozkan, F., & Unsal, M. (2007). On the Use of Venturi Tubes in Aeration. *CLEAN – Soil, Air, Water*, *35*(2), 183-185. https://doi.org/10.1002/clen.200600025

Baylar, A., Ozkan, F., & Unsal, M. (2010). Effect of air inlet hole diameter of venturi tube on air injection rate. *KSCE Journal Of Civil Engineering*, *14*(4), 489-492. https://doi.org/10.1007/s12205-010-0489-6

Behnisch, J., Ganzauge, A., Sander, S., Herrling, M., & Wagner, M. (2018). Improving aeration systems in saline water: measurement of local bubble size and volumetric mass transfer coefficient of conventional membrane diffusers. *Water Science and Technology*, *78*(4), 860-867. https://doi.org/10.2166/wst.2018.358

Beltrán, F. (2004). *Ozone reaction kinetics for water and wastewater systems*. Lewis Publishers.

Bezbarua, B., & Reckhow, D. (2004). Modification of the Standard Neutral Ozone Decomposition Model. *Ozone: Science & Engineering*, *26*(4), 345-357. https://doi.org/10.1080/01919510490482179

995 Bińk, A. (2013). Comments on “Decay of Ozone in Water: A Review” by D. Gardoni, A.
996 Vailati, and R. Canziani (Ozone: Science & Engineering, 34(4): 233–242). *Ozone: Science &*
997 *Engineering*, *35*(1), 3-5. https://doi.org/10.1080/01919512.2013.745060

998 Bredwell, M., & Worden, R. (1998). Mass-Transfer Properties of Microbubbles. 1.
999 Experimental Studies. *Biotechnology Progress*, *14*(1), 31-38.
1000 https://doi.org/10.1021/bp970133x

1001 Budhijanto, W., Deendarlianto, D., Kristiyani, H., & Satriawan, D. (2015). Enhancement of
1002 Aerobic Wastewater Treatment by the Application of Attached Growth Microorganisms and
1003 Microbubble Generator. *International Journal Of Technology*, *6*(7), 1101.
1004 https://doi.org/10.14716/ijtech.v6i7.1240

1005 Buxton, G., Greenstock, C., Helman, W., & Ross, A. (1988). Critical Review of rate
1006 constants for reactions of hydrated electrons, hydrogen atoms and hydroxyl radicals
1007 (·OH/·O−) in Aqueous Solution. *Journal of Physical and Chemical Reference Data*, *17*(2),
1008 513-886. https://doi.org/10.1063/1.555805

1009 Chedeville, O., Debacq, M., & Porte, C. (2009). Removal of phenolic compounds present in
1010 olive mill wastewaters by ozonation. *Desalination*, *249*(2), 865-869.
1011 https://doi.org/10.1016/j.desal.2009.04.014

1012 Cheng, W., Jiang, L., Quan, X., Cheng, C., Huang, X., Cheng, Z., & Yang, L. (2019).
1013 Ozonation process intensification of p-nitrophenol by in situ separation of hydroxyl radical
1014 scavengers and microbubbles. *Water Science and Technology*, *80*(1), 25-36.
1015 https://doi.org/10.2166/wst.2019.227

1016 Cheng, X., Xie, Y., Zheng, H., Yang, Q., Zhu, D., & Xie, J. (2016). Effect of the Different
1017 Shapes of Air Diffuser on Oxygen Mass Transfer Coefficients in Microporous Aeration

Systems. *Procedia Engineering*, *154*, 1079-1086. https://doi.org/10.1016/j.proeng.2016.07.599

Chiu, C., Chang, C., Chen, Y., Yu, Y., Chiang, P. and Ku, Y. (2003). Ozone mass transfer with combined effects of ozone decomposition and reaction with pollutants in a semibatch stirred vessel. *Journal of the Chinese Institute of Chemical Engineers*, *34*(3), 281-289.

Chu, L., Xing, X., Yu, A., Zhou, Y., Sun, X., & Jurcik, B. (2007). Enhanced ozonation of simulated dyestuff wastewater by microbubbles. *Chemosphere*, *68*(10), 1854-1860. https://doi.org/10.1016/j.chemosphere.2007.03.014

Chu, L., Yan, S., Xing, X., Yu, A., Sun, X., & Jurcik, B. (2008). Enhanced sludge solubilization by microbubble ozonation. *Chemosphere*, *72*(2), 205-212. https://doi.org/10.1016/j.chemosphere.2008.01.054

Clift, R., Grace, J., & Weber, M. (1978). *Bubbles, Drops, and Particles*. Academic Press.

da Silva Henauth, R., de Souza Vasconcelos, R., de Moura, A., Sarubbo, L., & dos Santos, V. (2016). Microbubble Generation with the Aid of a Centrifugal Pump. *Chemical Engineering & Technology*, *40*(1), 138-144. https://doi.org/10.1002/ceat.201500301

Deendarlianto, D., Wiratni, W., Tontowi, A. E., Indarto, I., & Iriawan, A. G. W. (2015). The Implementation of a Developed Microbubble Generator on the Aerobic Wastewater Treatment. *IJTech*, *6*(6), 924. https://doi.org/10.14716/ijtech.v6i6.1696

Deendarlianto, D., Indarto, I., Juwana, W., Afisna, L., & Nugroho, F. (2017). Performance of Porous-Venturi Microbubble Generator for Aeration Process. *Journal of Energy, Mechanical, Material and Manufacturing Engineering*, *2*(2). https://doi.org/10.22219/jemmme.v2i2.5054

Dehouli, H., Chedeville, O., Cagnon, B., Caqueret, V., & Porte, C. (2010). Influences of pH, temperature and activated carbon properties on the interaction ozone/activated carbon for a

wastewater treatment process. *Desalination*, *254*(1-3), 12-16. https://doi.org/10.1016/j.desal.2009.12.021

DeMoyer, C., Gulliver, J., & Wilhelms, S. (2001). Comparison of Submerged Aerator Effectiveness. *Lake and Reservoir Management*, *17*(2), 139-152. https://doi.org/10.1080/07438140109353982

Ershov, B., & Morozov, P. (2009). The kinetics of ozone decomposition in water, the influence of pH and temperature. *Russian Journal of Physical Chemistry A*, *83*(8), 1295-1299. https://doi.org/10.1134/s0036024409080093

Evans, H., Bauer, M., Luckman, I., & Page, M. (2003). An Assessment of the Benefits Afforded by the Continuous Versus Intermittent Operation of Ozone for Drinking Water Treatment. *Ozone: Science & Engineering*, *25*(5), 417-430. https://doi.org/10.1080/01919510390481748

Fábián, I. (2006). Reactive intermediates in aqueous ozone decomposition: A mechanistic approach. *Pure and Applied Chemistry*, *78*(8), 1559-1570. https://doi.org/10.1351/pac200678081559

Fuchun, X., & Cunli, L. (1990). Mass Balance Analysis of Ozone in a Conventional Bubble Column. *Ozone: Science & Engineering*, *12*(3), 269-279. https://doi.org/10.1080/01919519008552196

Gao, M., Hirata, M., Takanashi, H., & Hano, T. (2005). Ozone mass transfer in a new gas–liquid contactor–Karman contactor. *Separation and Purification Technology*, *42*(2), 145-149. https://doi.org/10.1016/j.seppur.2004.07.004

Gao, Y., Duan, Y., Fan, W., Guo, T., Huo, M., & Yang, W. *et al*. (2019). Intensifying ozonation treatment of municipal secondary effluent using a combination of microbubbles

and ultraviolet irradiation. *Environmental Science and Pollution Research*, *26*(21), 21915-21924. https://doi.org/10.1007/s11356-019-05554-8

Gardoni, D., Vailati, A., & Canziani, R. (2012). Decay of Ozone in Water: A Review. *Ozone: Science & Engineering*, *34*(4), 233-242. https://doi.org/10.1080/01919512.2012.686354

Garrido-Baserba, M., Asvapathanagul, P., Park, H., Kim, T., Baquero-Rodriguez, G., Olson, B., & Rosso, D. (2018). Impact of fouling on the decline of aeration efficiency under different operational conditions at WRRFs. *Science of The Total Environment*, *639*, 248-257. https://doi.org/10.1016/j.scitotenv.2018.05.036

Gurol, M., & Singer, P. (1982). Kinetics of ozone decomposition: a dynamic approach. *Environmental Science & Technology*, *16*(7), 377-383. https://doi.org/10.1021/es00101a003

Hanotu, J., Bandulasena, H., & Zimmerman, W. (2012). Microflotation performance for algal separation. *Biotechnology And Bioengineering*, *109*(7), 1663-1673. https://doi.org/10.1002/bit.24449

Hanotu, J., Karunakaran, E., Bandulasena, H., Biggs, C., & Zimmerman, W. (2014). Harvesting and dewatering yeast by microflotation. *Biochemical Engineering Journal*, *82*, 174-182. https://doi.org/10.1016/j.bej.2013.10.019

Hanotu, J., Kong, D., & Zimmerman, W. (2016). Intensification of yeast production with microbubbles. *Food and Bioproducts Processing*, *100*, 424-431. https://doi.org/10.1016/j.fbp.2016.07.013

Hanotu, J., Bandulasena, H., & Zimmerman, W. (2017). Aerator design for microbubble generation. *Chemical Engineering Research and Design*, *123*, 367-376. https://doi.org/10.1016/j.cherd.2017.01.034

1087 Haruta, K., & Takeyama, T. (1981). Kinetics of oxidation of aqueous bromide ion by
1088 ozone. *The Journal of Physical Chemistry*, *85*(16), 2383-2388.
1089 https://doi.org/10.1021/j150616a018

1090 Hoigné, J., & Bader, H. (1983). Rate constants of reactions of ozone with organic and
1091 inorganic compounds in water—I. *Water Research*, *17*(2), 173-183.
1092 https://doi.org/10.1016/0043-1354(83)90098-2

1093 Hoigné, J. (1994). Characterization of Water Quality Criteria for Ozonation Processes. Part I:
1094 Minimal Set of Analytical Data. *Ozone: Science & Engineering*, *16*(2), 113-120.
1095 https://doi.org/10.1080/01919519408552416

1096 Hongprasith, N., Dolkittikul, N., Apiboonsuwan, K., Pungrasmi, W., & Painmanakul, P.
1097 (2016). Study of different flexible aeration tube diffusers: Characterization and oxygen
1098 transfer performance. *Environmental Engineering Research*, *21*(3), 233-240.
1099 https://doi.org/10.4491/eer.2015.082

1100 Hu, L., & Xia, Z. (2018). Application of ozone micro-nano-bubbles to groundwater
1101 remediation. *Journal of Hazardous Materials*, *342*, 446-453.
1102 https://doi.org/10.1016/j.jhazmat.2017.08.030

1103 Hou, S., Jia, S., Jia, J., He, Z., Li, G., Zuo, Q. & Zhuang, H. (2020) Fe_3O_4 nanoparticles loading
1104 on cow dung based activated carbon as an efficient catalyst for catalytic microbubble ozonation
1105 of biologically pretreated coal gasification wastewater. *Journal of Environmental*
1106 *Management*, *267*,110615. https://doi.org/10.1016/j.jenvman.2020.110615

1107

1108 Huang, W., Chang, C., Chiu, C., Lee, S., Yu, Y., & Liou, H. *et al*. (1998). A refined model
1109 for ozone mass transfer in a bubble column. *Journal of Environmental Science and Health,*
1110 *Part A*, *33*(3), 441-460. https://doi.org/10.1080/10934529809376741

1111 Huang, X., Cheng, W., Quan, X., Cheng, C., Cheng, Z., & Yang, L. (2018). Catalytic
1112 Ozonation of Biologically Treated Leachate from Municipal Solid Waste in a Microbubble
1113 Reactor. *Ozone: Science & Engineering*, *41*(5), 415–426.
1114 https://doi.org/10.1080/01919512.2018.1555027

1115 Huang, X., Quan, X., Cheng, W., Cheng, C., Cheng, Z., Yang, L., & Jiang, L. (2019).
1116 Enhancement of Ozone Mass Transfer by Stainless Steel Wire Mesh and Its Effect on
1117 Hydroxyl Radical Generation. *Ozone: Science & Engineering*, 1-10.
1118 https://doi.org/10.1080/01919512.2019.1676196

1119 Hsu, Y., Chen, T., Chen, J., & Lay, C. (2002). Ozone Transfer into Water in a Gas-Inducing
1120 Reactor. *Industrial & Engineering Chemistry Research*, *41*(1), 120-127.
1121 https://doi.org/10.1021/ie0101341

1122 Ignatiev, A., Pryakhin, A., & Lunin, V. (2008). Numerical simulation of the kinetics of ozone
1123 decomposition in an aqueous solution. *Russian Chemical Bulletin*, *57*(6), 1172-1178.
1124 https://doi.org/10.1007/s11172-008-0146-0

1125 International Organization for Standardization (2017). *ISO/TC 281 - Fine bubble technology*.
1126 ISO. Retrieved 1 June 2020, from https://www.iso.org/committee/4856666.html.

1127 Jabesa, A., & Ghosh, P. (2016a). Removal of diethyl phthalate from water by ozone
1128 microbubbles in a pilot plant. *Journal of Environmental Management*, *180*, 476-484.
1129 https://doi.org/10.1016/j.jenvman.2016.05.072

1130 Jabesa, A., & Ghosh, P. (2016b). Removal of dimethyl phthalate from water by ozone
1131 microbubbles. *Environmental Technology*, *38*(16), 2093-2103.
1132 https://doi.org/10.1080/09593330.2016.1246610

1133 Jodzis, S., & Zięba, M. (2018). Energy efficiency of an ozone generation process in oxygen.
1134 Analysis of a pulsed DBD system. *Vacuum*, *155*, 29-37.
1135 https://doi.org/10.1016/j.vacuum.2018.05.035

1136 Joshi, M., & Shambaugh, R. (1982). The kinetics of ozone-phenol reaction in aqueous
1137 solutions. *Water Research*, *16*(6), 933-938. https://doi.org/10.1016/0043-1354(82)90025-2

1138 Juwana, W. E., Widyatama, A., Wiratni, Indarto, & Deendarlianto. (2018). *An evaluation of*
1139 *the horizontal injection microbubble generator*. https://doi.org/10.1063/1.5062742

1140 Juwana, W. E., Widyatama, A., Dinaryanto, O., Budhijanto, W., Indarto, & Deendarlianto.
1141 (2019). Hydrodynamic characteristics of the microbubble dissolution in liquid using orifice
1142 type microbubble generator. *Chemical Engineering Research and Design*, *141*, 436–448.
1143 https://doi.org/10.1016/j.cherd.2018.11.017

1144 Kamaroddin, M., Hanotu, J., Gilmour, D., & Zimmerman, W. (2016). In-situ disinfection and
1145 a new downstream processing scheme from algal harvesting to lipid extraction using ozone-
1146 rich microbubbles for biofuel production. *Algal Research*, *17*, 217-226.
1147 https://doi.org/10.1016/j.algal.2016.05.006

1148 Kamaroddin, M., Rahaman, A., Gilmour, D., & Zimmerman, W. (2020). Optimization and
1149 cost estimation of microalgal lipid extraction using ozone-rich microbubbles for biodiesel
1150 production. *Biocatalysis And Agricultural Biotechnology*, *23*, 101462.
1151 https://doi.org/10.1016/j.bcab.2019.101462

Kawahara, A., Sadatomi, M., Matsuyama, F., Matsuura, H., Tominaga, M., & Noguchi, M. (2009). Prediction of micro-bubble dissolution characteristics in water and seawater. *Experimental Thermal and Fluid Science, 33*(5), 883–894. https://doi.org/10.1016/j.expthermflusci.2009.03.004

Khuntia, S., Majumder, S., & Ghosh, P. (2012). Microbubble-aided water and wastewater purification: a review. *Reviews in Chemical Engineering*, *28*(4-6). https://doi.org/10.1515/revce-2012-0007

Khuntia, S., Majumder, S., & Ghosh, P. (2013). Removal of Ammonia from Water by Ozone Microbubbles. *Industrial & Engineering Chemistry Research*, *52*(1), 318-326. https://doi.org/10.1021/ie302212p

Khuntia, S., Majumder, S., & Ghosh, P. (2016). Catalytic ozonation of dye in a microbubble system: Hydroxyl radical contribution and effect of salt. *Journal of Environmental Chemical Engineering*, *4*(2), 2250-2258. https://doi.org/10.1016/j.jece.2016.04.005

Kong, S., Kwon, C., & Kim, M. (2003). Ozone kinetics and diesel decomposition by ozonation in groundwater. *Korean Journal of Chemical Engineering*, *20*(2), 293-299. https://doi.org/10.1007/bf02697244

Ku, Y., Su, W., & Shen, Y. (1996). Decomposition Kinetics of Ozone in Aqueous Solution. *Industrial & Engineering Chemistry Research*, *35*(10), 3369-3374. https://doi.org/10.1021/ie9503959

Kukuzaki, M., Fujimoto, K., Kai, S., Ohe, K., Oshima, T., & Baba, Y. (2010). Ozone mass transfer in an ozone–water contacting process with Shirasu porous glass (SPG) membranes—A comparative study of hydrophilic and hydrophobic membranes. *Separation and Purification Technology*, *72*(3), 347-356. https://doi.org/10.1016/j.seppur.2010.03.004

Kuo, P., Chian, E., & Chang, B. (1977). Identification of end products resulting from ozonation and chlorination of organic compounds commonly found in water. *Environmental Science & Technology*, *11*(13), 1177-1181. https://doi.org/10.1021/es60136a012

KTMindetail Of NIKUNI WEBSITE. (n.d.). NIKUNI WEBSITE. Retrieved October 8, 2020, from http://nikunijapan.com/ktm.html

Lage Filho, F. (2010). Ozone application in water sources: effects of operational parameters and water quality variables on ozone residual profiles and decay rates. *Brazilian Journal of Chemical Engineering*, *27*(4), 545-554. https://doi.org/10.1590/s0104-66322010000400006

Lee, Y., Park, Y., Lee, G., Kim, Y., & Chon, K. (2019). Enhanced Degradation of Pharmaceutical Compounds by a Microbubble Ozonation Process: Effects of Temperature, pH, and Humic Acids. *Energies*, *12*(22), 4373. https://doi.org/10.3390/en12224373

Levanov, A., Isaikina, O., Gasanova, R., & Lunin, V. (2017). Coefficient of ozone mass transfer during its interaction with an aqueous solution of formic acid in a bubble column reactor. *Russian Journal of Physical Chemistry A*, *91*(8), 1427-1431. https://doi.org/10.1134/s0036024417080167

Levitsky, I., Tavor, D., & Gitis, V. (2016). Generation of Two-Phase Air-Water Flow with Fine Microbubbles. *Chemical Engineering Technology*, *39*(8), 1537–1544. https://doi.org/10.1002/ceat.201500492

Li, P., & Tsuge, H. (2006). Ozone Transfer in a New Gas-Induced Contactor with Microbubbles. *Journal of Chemical Engineering of Japan / JCEJ*, *39*(11), 1213–1220. https://doi.org/10.1252/jcej.39.1213

Li, H., Hu, L., Song, D., & Al-Tabbaa, A. (2013a). Subsurface Transport Behavior of Micro-Nano Bubbles and Potential Applications for Groundwater Remediation. *IJERPH*, *11*(1), 473–486. https://doi.org/10.3390/ijerph110100473

Li, H., Hu, L., & Xia, Z. (2013b). Impact of Groundwater Salinity on Bioremediation Enhanced by Micro-Nano Bubbles. *Materials*, *6*(9), 3676–3687. https://doi.org/10.3390/ma6093676

Li, P., & Tsuge, H. (2006). Ozone Transfer in a New Gas-Induced Contactor with Microbubbles. *Journal of Chemical Engineering Of Japan*, *39*(11), 1213-1220. https://doi.org/10.1252/jcej.39.1213

Li, X., Li, P., Zu, L., & Yang, C. (2016). Gas-Liquid Mass Transfer Characteristics with Microbubble Aeration - I. Standard Stirred Tank. *Chem. Eng. Technol.*, *39*(5), 945–952. https://doi.org/10.1002/ceat.201500644

Lim, S., McArdell, C., & von Gunten, U. (2019). Reactions of aliphatic amines with ozone: Kinetics and mechanisms. *Water Research*, *157*, 514-528. https://doi.org/10.1016/j.watres.2019.03.089

Liu, S, Oshita, S., Kawabata, S., Makino, Y. & Yoshimoto, T. (2016). Identification of ROS produced by nanobubbles and their positive and negative effects on vegetable seed germination. *Langmuir*, *32*, 11295-11302. https://doi.org/10.1021/acs.langmuir.6b01621

Liu, C., Chen, X.-X., Zhang, J., Zhou, H.-Z., Zhang, L., & Guo, Y.-K. (2018). Advanced treatment of bio-treated coal chemical wastewater by a novel combination of microbubble catalytic ozonation and biological process. *Separation and Purification Technology*, *197*, 295–301. https://doi.org/10.1016/j.seppur.2018.01.005

Liu, C., Tanaka, H., Ma, J., Zhang, L., Zhang, J., Huang, X., & Matsuzawa, Y. (2012). Effect of microbubble and its generation process on mixed liquor properties of activated sludge using Shirasu porous glass (SPG) membrane system. *Water Research*, *46*(18), 6051-6058. https://doi.org/10.1016/j.watres.2012.08.032

Liu, C., Tanaka, H., Zhang, J., Zhang, L., Yang, J., Huang, X., & Kubota, N. (2013). Successful application of Shirasu porous glass (SPG) membrane system for microbubble aeration in a biofilm reactor treating synthetic wastewater. *Separation and Purification Technology*, *103*, 53-59. https://doi.org/10.1016/j.seppur.2012.10.023

Liu, S., Wang, Q., Zhai, X., Huang, Q., & Huang, P. (2010). Improved Pretreatment (Coagulation-Floatation and Ozonation) of Younger Landfill Leachate by Microbubbles. *Water Environment Research*, *82*(7), 657-665. https://doi.org/10.2175/106143010x12609736966522

López-López, A., Pic, J., & Debellefontaine, H. (2007). Ozonation of azo dye in a semi-batch reactor: A determination of the molecular and radical contributions. *Chemosphere*, *66*(11), 2120-2126. https://doi.org/10.1016/j.chemosphere.2006.09.025

Lovato, M., Martín, C., & Cassano, A. (2009). A reaction kinetic model for ozone decomposition in aqueous media valid for neutral and acidic pH. *Chemical Engineering Journal*, *146*(3), 486-497. https://doi.org/10.1016/j.cej.2008.11.001

Magara, Y., Itoh, M., & Morioka, T. (1995). Application of ozone to water treatment and power consumption of ozone generating systems. *Progress in Nuclear Energy*, *29*, 175-182. https://doi.org/10.1016/0149-1970(95)00041-h

Majid, A., Deendarlianto, Wiratni, Indarto, Enggar, B., Baskoro, P & Alva T., (2016). Development of an Industrial-Scale Micro-bubble Generator for the Purposes of Aerobic

Wastewater Treatment. *The 9th International Conference on Multiphase Flow*. 10.13140/RG.2.1.2618.5203.

Majid, A., Nugroho, F., Juwana, W., Budhijanto, W., Deendarlianto, & Indarto. (2018). On the performance of venturi-porous pipe microbubble generator with inlet angle of 20° and outlet angle of 12°. https://doi.org/10.1063/1.5050000

Merle, T., Pronk, W., & von Gunten, U. (2017). MEMBRO3X, a Novel Combination of a Membrane Contactor with Advanced Oxidation (O3/H2O2) for Simultaneous Micropollutant Abatement and Bromate Minimization. *Environmental Science & Technology Letters*, *4*(5), 180-185. https://doi.org/10.1021/acs.estlett.7b00061

Miklos, D.B., Remy, C., Jekel, M., Linden, K., Drewes, J.E., Hübner, U. (2018). Evaluation of advanced oxidation processes for water and wastewater treatment – A critical review. *Water Research*, 139, 118-131. https://doi.org/10.1016/j.watres.2018.03.042

Mitani, M., Keller, A., Sandall, O., & Rinker, R. (2005). Mass Transfer of Ozone Using a Microporous Diffuser Reactor System. *Ozone: Science & Engineering*, *27*(1), 45-51. https://doi.org/10.1080/01919510590908995

Morooka, S., K. Ikezumi, and Y. Kato. (1978). The Decomposition of Ozone in Aqueous Solution. *International Journal of Chemical Engineering*, *19*, 355.

Mueller, J., Boyle, W., & Pöpel, H. (2002). *Aeration*. CRC Press.

Muroyama, K., Imai, K., Oka, Y., & Hayashi, J. (2013). Mass transfer properties in a bubble column associated with micro-bubble dispersions. *Chemical Engineering Science*, *100*, 464-473. https://doi.org/10.1016/j.ces.2013.03.043

Muruganandham, M., Suri, R., Jafari, S., Sillanpää, M., Lee, G., Wu, J., & Swaminathan, M. (2014). Recent Developments in Homogeneous Advanced Oxidation Processes for Water and

Wastewater Treatment. *International Journal of Photoenergy*, *2014*, 1-21. https://doi.org/10.1155/2014/821674

Nam, G., Mohamed, M., & Jung, J. (2019). Enhanced degradation of benzo[a]pyrene and toxicity reduction by microbubble ozonation. *Environmental Technology*, 1-8. https://doi.org/10.1080/09593330.2019.1683077

Neta, P., & Dorfman, L. (1968). Pulse-radiolysis studies. XIII. Rate constants for the reactions of hydroxyl radicals with aromatic compounds in aqueous solutions. *Advances In Chemistry*, *81*(15), 222-230.

Paucar, N., Kim, I., Tanaka, H., & Sato, C. (2018). Ozone treatment process for the removal of pharmaceuticals and personal care products in wastewater. *Ozone: Science & Engineering*, *41*(1), 3-16. https://doi.org/10.1080/01919512.2018.1482456

Park, S., Park, C., Lee, J., & Lee, B. (2017). A Simple Parameterization for the Rising Velocity of Bubbles in a Liquid Pool. *Nuclear Engineering and Technology*, *49*(4), 692-699. https://doi.org/10.1016/j.net.2016.12.006

Parkinson, L., Sedev, R., Fornasiero, D., & Ralston, J. (2008). The terminal rise velocity of 10–100 μm diameter bubbles in water. *Journal of Colloid and Interface Science*, *322*(1), 168-172. https://doi.org/10.1016/j.jcis.2008.02.072

Parmar, R., & Majumder, S. (2013). Microbubble generation and microbubble-aided transport process intensification—A state-of-the-art report. *Chemical Engineering and Processing: Process Intensification*, *64*, 79-97. https://doi.org/10.1016/j.cep.2012.12.002

Rahman, A., Darban Ahmad, K., Mahmoud, A., & Maoming, F. (2014). Nano-microbubble flotation of fine and ultrafine chalcopyrite particles. *International Journal of Mining Science and Technology* , *24*(4), 559–566. https://doi.org/10.1016/j.ijmst.2014.05.021

Rakness, K., Hunter, G., Lew, J., Mundy, B., & Wert, E. (2018). Design Considerations for Cost-Effective Ozone Mass Transfer in Sidestream Systems. *Ozone: Science & Engineering*, *40*(3), 159-172. https://doi.org/10.1080/01919512.2018.1424532

Rehman, F., Medley, G., Bandulasena, H., & Zimmerman, W. (2015). Fluidic oscillator-mediated microbubble generation to provide cost effective mass transfer and mixing efficiency to the wastewater treatment plants. *Environmental Research*, *137*, 32-39. https://doi.org/10.1016/j.envres.2014.11.017

Rischbieter, E., Stein, H., & Schumpe, A. (2000). Ozone Solubilities in Water and Aqueous Salt Solutions. *Journal of Chemical & Engineering Data*, *45*(2), 338-340. https://doi.org/10.1021/je990263c

Roustan, M., Wang, R., & Wolbert, D. (1996). Modeling Hydrodynamics and Mass Transfer Parameters In A Continuous Ozone Bubble Column. *Ozone: Science & Engineering*, *18*(2), 99-115. https://doi.org/10.1080/01919519608547331

Sadatomi, M., Kawahara, A., Kano, K., & Ohtomo, A. (2005). Performance of a new micro-bubble generator with a spherical body in a flowing water tube. *Experimental Thermal and Fluid Science*, *29*(5), 615-623. https://doi.org/10.1016/j.expthermflusci.2004.08.006

Sadatomi, M., Kawahara, A., Matsuyama, F., & Kimura, T. (2007). An advanced microbubble generator and its application to a newly developed bubble-jet-type air-lift pump. *MultScienTechn*, *19*(4), 323–342. https://doi.org/10.1615/multscientechn.v19.i4.20

Sadatomi, M., Kawahara, A., Matsuura, H., & Shikatani, S. (2012). Micro-bubble generation rate and bubble dissolution rate into water by a simple multi-fluid mixer with orifice and porous tube. *Experimental Thermal and Fluid Science*, *41*, 23-30. https://doi.org/10.1016/j.expthermflusci.2012.03.002

Santana, M., Zhang, Q., & Mihelcic, J. (2014). Influence of Water Quality on the Embodied Energy of Drinking Water Treatment. *Environmental Science & Technology*, *48*(5), 3084-3091. https://doi.org/10.1021/es404300y

Sein, M., Golloch, A., Schmidt, T., & von Sonntag, C. (2007). No Marked Kinetic Isotope Effect in the Peroxone (H2O2/D2O2+O3) Reaction: Mechanistic Consequences. *Chemphyschem*, *8*(14), 2065-2067. https://doi.org/10.1002/cphc.200700493

Shangguan, Y., Yu, S., Gong, C., Wang, Y., Yang, W., & Hou, L. (2018). A Review of Microbubble and its Applications in Ozonation. *IOP Conference Series: Earth and Environmental Science*, *128*, 012149. https://doi.org/10.1088/1755-1315/128/1/012149

Shin, W., Mirmiran, A., Yiacoumi, S., & Tsouris, C. (1999). Ozonation using microbubbles formed by electric fields. *Separation and Purification Technology*, *15*(3), 271-282. https://doi.org/10.1016/s1383-5866(98)00107-5

Sotelo, J., Beltran, F., Benitez, F., & Beltran-Heredia, J. (1987). Ozone decomposition in water: kinetic study. *Industrial & Engineering Chemistry Research*, *26*(1), 39-43. https://doi.org/10.1021/ie00061a008

Sun, L., Mo, Z., Zhao, L., Liu, H., Guo, X., Ju, X., & Bao, J. (2017). Characteristics and mechanism of bubble breakup in a bubble generator developed for a small TMSR. *Annals of Nuclear Energy*, *109*, 69–81. https://doi.org/10.1016/j.anucene.2017.05.015

Sun, Z., Chen, X., Yang, K., Zhu, N., & Lou, Z. (2020). The progressive steps for TPH stripping and the decomposition of oil refinery sludge using microbubble ozonation. *Science Of The Total Environment*, *712*, 135631. https://doi.org/10.1016/j.scitotenv.2019.135631

1331 Suwartha, N., Syamzida, D., Priadi, C., Moersidik, S., & Ali, F. (2020). Effect of size
1332 variation on microbubble mass transfer coefficient in flotation and aeration
1333 processes. *Heliyon*, *6*(4), e03748. https://doi.org/10.1016/j.heliyon.2020.e03748

1334 Takahashi, M., Chiba, K., & Li, P. (2007). Formation of Hydroxyl Radicals by Collapsing
1335 Ozone Microbubbles under Strongly Acidic Conditions. *The Journal of Physical Chemistry*
1336 *B*, *111*(39), 11443-11446. https://doi.org/10.1021/jp074727m

1337 Takahashi, N., Ichikawa, H., Torii, H., Shibata, S., Duy, N., & Phuong, P. (2012a). Ozonation
1338 of Dyestuff Solutions Using a Fine Bubble Generator System. *Ozone: Science &*
1339 *Engineering*, *34*(3), 196-203. https://doi.org/10.1080/01919512.2012.663720

1340 Takahashi, M., Ishikawa, H., Asano, T., & Horibe, H. (2012b). Effect of Microbubbles on
1341 Ozonized Water for Photoresist Removal. *The Journal of Physical Chemistry C*, *116*(23),
1342 12578-12583. https://doi.org/10.1021/jp301746g

1343 Talaia, M. (2007). Terminal velocity of a bubble rise in a liquid column. *World Academy of*
1344 *Science, Engineering and Technology*, *22*, 264-268.

1345 Tanaka, S., Kastens, S., Fujioka, S., Schlüter, M., & Terasaka, K. (2020). Mass transfer from
1346 freely rising microbubbles in aqueous solutions of surfactant or salt. *Chemical Engineering*
1347 *Journal*, *387*, 121246. https://doi.org/10.1016/j.cej.2019.03.122

1348 Tang, G., Adu-Sarkodie, K., Kim, D., Kim, J., Teefy, S., Shukairy, H., & Mariñas, B. (2005).
1349 Modeling Cryptosporidium parvum oocyst Inactivation and bromate formation in a full-scale
1350 ozone contactor. *Environmental Science & Technology*, *39*(23), 9343-9350.
1351 https://doi.org/10.1021/es050345n

1352 Tekle-Röttering, A., Lim, S., Reisz, E., Lutze, H., Abdighahroudi, M., & Willach, S. *et al*.
1353 (2020). Reactions of pyrrole, imidazole, and pyrazole with ozone: kinetics and

mechanisms. *Environmental Science: Water Research & Technology*, *6*(4), 976-992. https://doi.org/10.1039/c9ew01078e

Temesgen, T., Bui, T., Han, M., Kim, T., & Park, H. (2017). Micro and nanobubble technologies as a new horizon for water-treatment techniques: A review. *Advances in Colloid And Interface Science*, *246*, 40-51. https://doi.org/10.1016/j.cis.2017.06.011

Terasaka, K., Hirabayashi, A., Nishino, T., Fujioka, S., & Kobayashi, D. (2011). Development of microbubble aerator for waste water treatment using aerobic activated sludge. *Chemical Engineering Science*, *66*(14), 3172-3179. https://doi.org/10.1016/j.ces.2011.02.043

Terashima, M., So, M., Goel, R., & Yasui, H. (2016). Determination of diffuser bubble size in computational fluid dynamics models to predict oxygen transfer in spiral roll aeration tanks. *Journal Of Water Process Engineering*, *12*, 120-126. https://doi.org/10.1016/j.jwpe.2016.07.001

Tizaoui, C., & Zhang, Y. (2010). The modelling of ozone mass transfer in static mixers using Back Flow Cell Model. *Chemical Engineering Journal*, *162*(2), 557-564. https://doi.org/10.1016/j.cej.2010.05.061

Uhm, H., Hong, Y., Lee, H., & Park, Y. (2009). Increase in the ozone decay time in acidic ozone water and its effects on sterilization of biological warfare agents. *Journal Of Hazardous Materials*, *168*(2-3), 1595-1601. https://doi.org/10.1016/j.jhazmat.2009.03.056

Valdés, H., Farfán, V., Manoli, J., & Zaror, C. (2009). Catalytic ozone aqueous decomposition promoted by natural zeolite and volcanic sand. *Journal of Hazardous Materials*, *165*(1-3), 915-922. https://doi.org/10.1016/j.jhazmat.2008.10.093

von Gunten, U., Elovitz, M., & Kaiser, H. (1999). Calibration of full-scale ozonation systems with conservative and reactive tracers. *Journal of Water Supply: Research And Technology—AQUA*, *48*(6), 250-256. https://doi.org/10.2166/aqua.1999.0027

von Sonntag, C. (2008). Advanced oxidation processes: mechanistic aspects. *Water Science and Technology*, *58*(5), 1015-1021.

Vyong Tkhi, L., Tarasov, V., & Popov, Y. (2009). The influence of traces on kinetics of ozone destruction in water. *Theoretical Foundations of Chemical Engineering*, *43*(5), 846-849. https://doi.org/10.1134/s0040579509050418

Wagner, M., & Pöpel, H. (1998). Oxygen transfer and aeration efficiency - influence of diffuser submergence, diffuser density, and blower type. *Water Science and Technology*, *38*(3), 1-6. https://doi.org/10.2166/wst.1998.0163

Wang, D., Yang, X., Tian, C., Lei, Z., Kobayashi, N., & Kobayashi, M. *et al*. (2019). Characteristics of ultra-fine bubble water and its trials on enhanced methane production from waste activated sludge. *Bioresource Technology*, *273*, 63-69. https://doi.org/10.1016/j.biortech.2018.10.077

Wang, W., Fan, W., Huo, M., Zhao, H., & Lu, Y. (2018). Hydroxyl Radical Generation and Contaminant Removal from Water by the Collapse of Microbubbles Under Different Hydrochemical Conditions. *Water, Air, & Soil Pollution*, *229*(3). https://doi.org/10.1007/s11270-018-3745-x

Wolf, C., Pavese, A., von Gunten, U., & Kohn, T. (2019). Proxies to monitor the inactivation of viruses by ozone in surface water and wastewater effluent. *Water Research*, *166*, 115088. https://doi.org/10.1016/j.watres.2019.115088

1398 Wu, C., Li, P., Xia, S., Wang, S., Wang, Y., & Hu, J. *et al*. (2019). The role of interface in
1399 microbubble ozonation of aromatic compounds. *Chemosphere, 220,* 1067-1074.
1400 https://doi.org/10.1016/j.chemosphere.2018.12.174

1401 Wu, Z., Shen, H., Ondruschka, B., Zhang, Y., Wang, W., & Bremner, D. (2012). Removal of
1402 blue-green algae using the hybrid method of hydrodynamic cavitation and ozonation. *Journal*
1403 *of Hazardous Materials, 235-236,* 152-158. https://doi.org/10.1016/j.jhazmat.2012.07.034

1404 Xu, X., Ge, X., Qian, Y., Zhang, B., Wang, H., & Yang, Q. (2018). Effect of nozzle diameter
1405 on bubble generation with gas self-suction through swirling flow. *Chemical Engineering*
1406 *Research and Design, 138,* 13–20. https://doi.org/10.1016/j.cherd.2018.04.027

1407 Xu, Z., Mochida, K., Naito, T., & Yasuda, K. (2012). Effects of Operational Conditions on
1408 1,4-Dioxane Degradation by Combined Use of Ultrasound and Ozone
1409 Microbubbles. *Japanese Journal of Applied Physics, 51,* 07GD08.
1410 https://doi.org/10.1143/jjap.51.07gd08

1411 Yamashita, T., & Ando, K. (2017). Aeration of water with oxygen microbubbles and its
1412 purging effect. *J. Fluid Mech., 825,* 16–28. https://doi.org/10.1017/jfm.2017.376

1413 Yao, K., Chi, Y., Wang, F., Yan, J., Ni, M., & Cen, K. (2016). *The effect of microbubbles on*
1414 *gas-liquid mass transfer coefficient and degradation rate of COD in wastewater treatment.*
1415 *73*(8), 1969–1977. https://doi.org/10.2166/wst.2016.018

1416 Zhang, J., Tejada-Martínez, A., Zhang, Q., & Lei, H. (2014). Evaluating hydraulic and
1417 disinfection efficiencies of a full-scale ozone contactor using a RANS-based modeling
1418 framework. *Water Research, 52,* 155-167. https://doi.org/10.1016/j.watres.2013.12.037

1419 Zhang, F., Xi, J., Huang, J., & Hu, H. (2013). Effect of inlet ozone concentration on the
1420 performance of a micro-bubble ozonation system for inactivation of Bacillus subtilis

spores. *Separation and Purification Technology*, *114*, 126-133. https://doi.org/10.1016/j.seppur.2013.04.034

Zhang, J., Huang, G., Liu, C., Zhang, R., Chen, X., & Zhang, L. (2018). Synergistic effect of microbubbles and activated carbon on the ozonation treatment of synthetic dyeing wastewater. *Separation and Purification Technology*, *201*, 10-18. https://doi.org/10.1016/j.seppur.2018.02.003

Zheng, T., Wang, Q., Zhang, T., Shi, Z., Tian, Y., & Shi, S. *et al*. (2015). Microbubble enhanced ozonation process for advanced treatment of wastewater produced in acrylic fiber manufacturing industry. *Journal of Hazardous Materials*, *287*, 412-420. https://doi.org/10.1016/j.jhazmat.2015.01.069

Zimmerman, W., Tesař, V., Butler, S., & Bandulasena, H. (2008). Microbubble Generation. *Recent Patents on Engineering*, *2*(1), 1-8. https://doi.org/10.2174/187221208783478598

Zimmerman, W., Zandi, M., Hemaka Bandulasena, H., Tesař, V., James Gilmour, D., & Ying, K. (2011a). Design of an airlift loop bioreactor and pilot scales studies with fluidic oscillator induced microbubbles for growth of a microalgae Dunaliella salina. *Applied Energy*, *88*(10), 3357-3369. https://doi.org/10.1016/j.apenergy.2011.02.013

Zimmerman, W., Tesař, V. & Hemaka Bandulasena, H. (2011b). Towards energy efficient nanobubble generation with fluidic oscillation. *Current Opinion in Colloid and Interface Science*, *16* (4), 350-356, https://doi.org/10.1016/j.cocis.2011.01.010

https://dspace.org/

Microbubbles and their application to ozonation in water treatment: A critical review exploring their benefit and future application

Alexander, John; Brookes, Adam; Carra, Irene; Jefferson, Bruce; Jarvis, Peter

2020-12-22
Taylor & Francis
https://doi.org/10.1080/10643389.2020.1860406
John A, Brookes A, Carra I, et al., (2022) Microbubbles and their application to ozonation in water treatment: A critical review exploring their benefit and future application. Critical Reviews in Environmental Science and Technology, Volume 52, Issue 9, September 2022, pp. 1561-1603

Downloaded from a DSpace repository. https://dspace.org/